

Review article

Biomedical applications of magnetosomes: State of the art and perspectives



Gang Ren^{a,b,1}, Xia Zhou^{a,c,1}, Ruimin Long^c, Maobin Xie^{d,e}, Ranjith Kumar Kankala^{c,f},
Shibin Wang^{a,b,f}, Yu Shrike Zhang^{d,**}, Yuangang Liu^{a,c,f,*}

^a Institute of Pharmaceutical Engineering, Huaqiao University, Xiamen, Fujian, 361021, China

^b College of Materials Science and Engineering, Huaqiao University, Xiamen, Fujian, 361021, China

^c College of Chemical Engineering, Huaqiao University, Xiamen, Fujian, 361021, China

^d Division of Engineering in Medicine, Department of Medicine, Brigham and Women's Hospital, Harvard Medical School, Cambridge, MA, 02139, USA

^e The Sixth Affiliated Hospital of Guangzhou Medical University, Qingyuan People's Hospital, School of Biomedical Engineering, Guangzhou Medical University, Guangzhou, 511436, China

^f Fujian Provincial Key Laboratory of Biochemical Technology, Xiamen, Fujian, 361021, China

ARTICLE INFO

Keywords:

Magnetosome
Bionic magnetosomes
Magnetotactic bacteria
Modification strategies
Biomedical applications

ABSTRACT

Magnetosomes, synthesized by magnetotactic bacteria (MTB), have been used in nano- and biotechnological applications, owing to their unique properties such as superparamagnetism, uniform size distribution, excellent bioavailability, and easily modifiable functional groups. In this review, we first discuss the mechanisms of magnetosome formation and describe various modification methods. Subsequently, we focus on presenting the biomedical advancements of bacterial magnetosomes in biomedical imaging, drug delivery, anticancer therapy, biosensor. Finally, we discuss future applications and challenges. This review summarizes the application of magnetosomes in the biomedical field, highlighting the latest advancements and exploring the future development of magnetosomes.

1. Introduction

Due to their unique magnetic responsiveness, magnetic nanoparticles have been widely used in diverse biomedical applications, such as detection, separation, drug delivery, and imaging, among others [1, 2]. However, chemically synthesized are often potentially biotoxic, requiring further modification. Although encapsulating magnetic nanoparticles in polymers improves safety considerations, their dispersibility must be increased using various surface active agents. These post-processing steps limit the large-scale utility of magnetic nanoparticles. Natural and bionic materials have attracted significant attention from researchers to address these problems. Magnetotactic bacteria (MTB), a special type of bacteria containing magnetosomes in their bodies, can respond to the magnetic field and move along the magnetic line of force. Therefore, the discovery of such native magnetic nanoparticles has attracted the attention of researchers, and with their favorable performances, it is expected that these natural magnetic nanoparticles could replace or supplement the traditional synthetic ones

in the biomedical field in the future.

Magnetosomes are intracellular organelles in magnetotactic bacteria (MTB). They generally contain magnetite (Fe_3O_4) or greigite (Fe_3S_4) particles surrounded by a proteolipidic membrane [3,4], and they are arranged in separate or multiple chains or dispersed in MTB. Although Bellini discovered that 'magnetosensitive bacteria' presented an internal 'magnetic compass' in 1963 [5], magnetosomes could not be confirmed until 1975, when Blakemore demonstrated their presence using transmission electron microscopy [6]. Compared with chemically synthesized magnetic nanoparticles, magnetosomes have a homogeneous morphology, a narrow size distribution, good dispersion, and favorable biocompatibility. Therefore, magnetosomes have attracted significant attention from researchers in recent years, focusing on the mechanism by which magnetosomes form, how they could be isolated, and potential biomedical applications. Magnetosomes have been applied to various processes, such as separation of molecules [7–9], immobilization [10], magnetic resonance imaging (MRI) [11], drug delivery [12,13], gene therapy [14,15], and hyperthermia therapy [16]. Moreover, biomimetic magnetosomes based on the structure of natural magnetosomes show

Peer review under responsibility of KeAi Communications Co., Ltd.

* Corresponding author. Institute of Pharmaceutical Engineering, Huaqiao University, Xiamen, Fujian, 361021, China.

** Corresponding author.

E-mail addresses: yszhang@research.bwh.harvard.edu (Y.S. Zhang), ygliu@hqu.edu.cn (Y. Liu).

¹ These authors contributed equally to this work.

<https://doi.org/10.1016/j.bioactmat.2023.04.025>

Received 17 January 2023; Received in revised form 12 April 2023; Accepted 29 April 2023

2452-199X/© 2023 The Authors. Publishing services by Elsevier B.V. on behalf of KeAi Communications Co. Ltd. This is an open access article under the CC BY-NC-ND license (<http://creativecommons.org/licenses/by-nc-nd/4.0/>).

Abbreviation			
MTB	Magnetotactic bacteria	PEI	Polyethyleneimine
BMs	Bacteria magnetosomes	DOX	Doxorubicin
MNPs	Magnetic nanoparticles	Ara-c;	Arabinoside
Fe ₃ O ₄	Magnetite	DNR	Daunorubicin
Fe ₃ S ₄	Greigite	AFenPs	amorphous iron nanoparticles
RBP	Red fluorescent protein	AMF	Alternating magnetic field
IPTG	Isopropyl β-D-1-thiogalactopyranoside	CDT	Chemodynamic therapy
sfGFP	Super folder green fluorescent protein	N-PLL;	Poly L-lysine
AFB1	Aflatoxin B1	N-CA	Citric acid
EDC	1-ethyl-3-[3-dimethylamino-propyl] carbodiimide	N-OA	Oleic acid
MTT	methylthiazolyl-diphenyl-tetrazolium bromide	N-CMG	Carboxymethyl glucan
MRI	Magnetic resonance imaging	PTT	Photothermal therapy
MPI	Magnetic particle imaging	pMHC-1	Histocompatibility complex class I
PET	Positron tomography	αCD28	Co-stimulatory ligand anti-CD28
SPECT	single photon emission computed tomography	DBCO	Dibenzocyclooctyne
DC	Direct current	SEB	Staphylococcal enterotoxin B
AC	Alternating current	HBsAg	hepatitis B surface antigen
RGD	Arginine-glycine-aspartic acid	PEF	Pefloxacin
PLGA	Polylactic-co-glycolic acid	MC-LR	Microcystin LR
APTES	3-aminopropyltriethoxysilane	GNRs	Gold nanorods
		OVA	Antigen-ovalbumin
		LSPR	Longitudinal surface plasmon resonance

excellent application potentials in the field of biomedicine. The magnetosome-like structure is often constructed by wrapping the cell membrane around the magnetic core. For example, Xiong et al. constructed bionic magnetosomes to enrich the circulating tumor cells in the blood by covering a layer of white blood cell membrane fragments on the surface of Fe₃O₄ magnetic nanoclusters through electrostatic interactions [17]. Although many aspects of magnetosomes have been presented – such as the mechanism of biomineralization, the isolation methods, and the constitution of the proteolipidic membrane – the applications of magnetosomes in biomedical science are still in the nascent stage due to the lack of exploration of their functional designs. In addition, because most magnetotactic bacteria have strict requirements for nutrition and environmental conditions, their artificial cultivation is difficult, resulting in the challenge of producing magnetosomes on a large scale. This factor also hinders the scalable applications of magnetosomes.

Our continuous research on magnetosomes since 2009 has inspired us to provide an overview of the recent advances in applying magnetosomes in the biomedical area, starting from a brief introduction of the

mechanism by which magnetosomes are formed, followed by a summary of functionalization methods of magnetosomes. Then, we highlight and discuss their recent biomedical applications based on advanced modifications. Finally, we highlight the future development potentials and challenges.

2. Bioproduction of magnetosomes

Due to the complex reaction process, uneven particle size and distribution, and difficulty in controlling the crystal form, chemically synthesized magnetic nanoparticles face many challenges in practical applications. To this end, magnetosomes can avoid these disadvantages. However, improving the production of magnetosomes has become a significant challenge for the large-scale utilities of magnetosomes.

Magnetotactic bacteria are widely distributed in nature. Since Blakemore et al. first proposed the large-scale culture method of *Magnetospirillum Magnetotacticum MS-1* in 1979 [18], researchers across the globe have carried out many studies on improving the production of magnetosomes (Fig. 1). The conditions required to obtain a high yield of

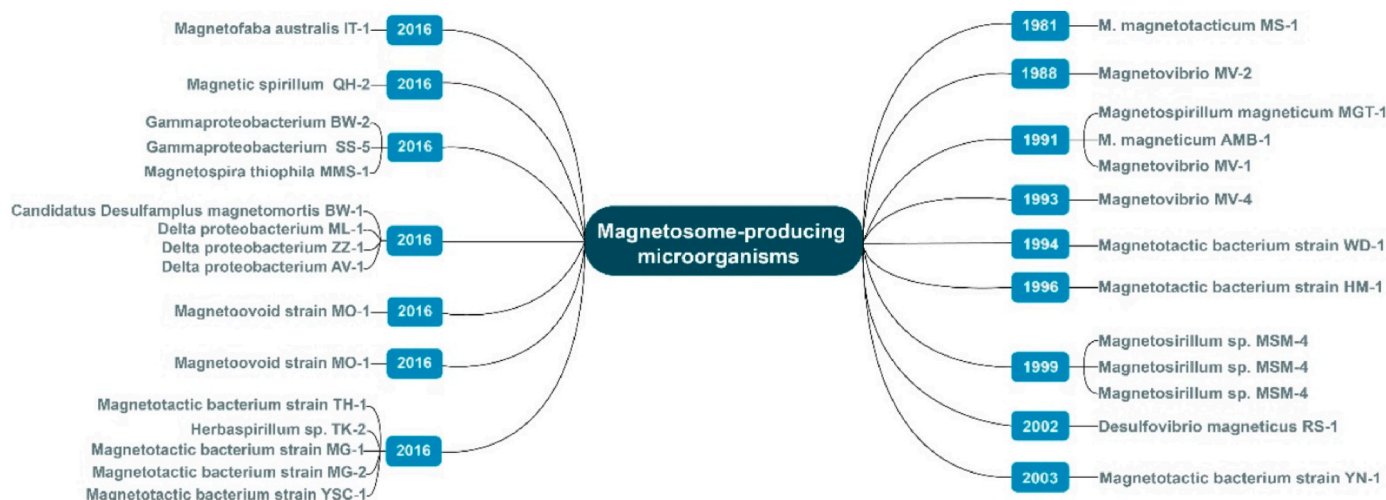


Fig. 1. Isolated and purified magnetotactic bacteria.

magnetosomes include a micro-aerobic or anaerobic environment, as well as appropriate sources and concentrations of carbon, nitrogen, and iron (such as ferric citrate and ferric quinate). Heyen and Schuler reported that the production yield of magnetosomes (6.3 mg of magnetite $L^{-1} day^{-1}$) was achieved by culturing *Magnetospirillum gryphiswaldense* at 25 mbar pO_2 [19]. Zhang et al. adopted a semi-continuous fermentation method that could provide nutrient balance and isotonic conditions for a high-density culture of MSR-1. After optimization of fermentation and culture conditions, the yield of magnetosomes was significantly increased to 168.3 and 83.5 mg/L/day at 36 h and 73 h, respectively [20]. Fernández-Castané et al. used the pH-stat feeding batch growth strategy to optimize the concentration of carbon source (lactic acid) and replaceable electron acceptor (sodium nitrate) in the medium. The highest biomass concentration and cellular iron content at 565 nm were 15.5 and 33.1 mg iron g^{-1} (dry cell weight), respectively [21]. Berny et al. explored the synthesis of high-purity magnetosomes to reduce the biological toxicity of magnetosomes. They used MSR-1 to find the minimum growth medium of the bacteria and pre-amplified it by feeding them with an iron source to synthesize high-purity magnetosomes (the mass percentage of iron was 99.8%) [22].

Currently, the purification and cultivation of magnetotactic bacteria and the improvement of magnetosome production are the key points in magnetosome research. In addition, other key steps include the large-scale production of magnetosomes with better performance and increased yield by optimizing and exploring the culture conditions of magnetotactic bacteria.

3. Formation mechanism of magnetosomes

Magnetosomes, formed by MTB, are composed of Fe_3O_4 or Fe_3S_4 nanocrystals enveloped by a phospholipid bilayer. The intracellular magnetic particles in MTB allow them to align passively along magnetic field lines, a behavior termed magnetotaxis [23]. Most MTB can produce nano-sized magnetite or greigite when cultivated in microaerophilic conditions. The magnetosomes possess an average size of 25–100 nm, and various crystal forms, including cubic octahedron, long rhombus, bullet head and other crystal forms. In addition, magnetosomes are distributed in the magnetosome membrane either in single or multiple chains. The magnetosome membrane plays a crucial role in the synthesis and applicability of magnetosomes providing an excellent biochemical environment for the biomineralization of magnetosomes. In addition, the specific proteins on its membrane make the magnetosomes exhibit bacterial specificity (Table 1).

In most MTB, magnetosome biosynthesis involves a complex gene island with a high guanine and cytosine (GC) content and rich in transfer RNA (tRNA) genes, pseudogenes, integrases, transposases, and transposon sequences. This specific gene island precisely regulates the biosynthetic process, thus conferring superior properties to magnetosomes. Most genes in gene land exist in the form of operons, such as *MamAB*, *MamXY*, *Mms6*, and *FeoAB1*, which play key roles in magnetosome biosynthesis. The main steps of biosynthesis are described below (Fig. 2) [24,25].

(1) Formation of the magnetosome membrane: This stage mainly includes the recruitment and storage of membrane proteins, the invagination of the cell plasma membrane, and the formation of the magnetosome membrane. The invagination process of the magnetosomes membrane can occur in multiple regions of the cell plasma membrane. Related proteins (such as *MamM*, *MamL*, *MamI*, *MamQ*, and *MamY*) and operons (such as *mamAB*, *mamGFDC*, and *mms6*) can induce the invagination and bending of the membrane as well as maintain the stability of the structure through the interaction between protein molecules [26]. Then, the recruitment of functional proteins further triggers the interaction and localization between proteins, activating the magnetosome biomineralization process. [27].

Table 1

A list of proteins from MTB related to magnetosome formation.

Function	Protein	Molecular weight (kDa)	
Membrane invagination	<i>MamB</i>	31.9	
	<i>MamM</i>	34.5	
	<i>MamL</i>	8.6	
	<i>MamI</i>	7.2	
	<i>MamQ</i>	30	
	<i>MamY</i>	40.9	
	<i>MamU</i>	32	
	<i>Mms16</i>	16.4	
	<i>MamE</i>	73.5	
	<i>MamC</i>	12.4	
	<i>MamF</i>	12.3	
	Protein recruitment	<i>MamA</i>	46.8
	Iron transport	<i>MamB</i>	31.9
<i>MamM</i>		34.5	
<i>MamH</i>		45.7	
<i>MamZ</i>		70.5	
<i>MamT</i>		18.9	
Iron oxidation and reduction	<i>MamZ</i>	70.5	
	<i>MamP</i>	29	
	<i>MamT</i>	18.9	
	<i>MamX</i>	28.2	
	<i>MamE</i>	73.5	
Function	Protein	Molecular weight (kDa)	
Crystal nucleation	<i>MamE</i>	73.5	
	<i>MamM</i>	34.5	
	<i>MamO</i>	66.3	
Crystal growth	<i>Mms5</i>	5.79	
	<i>Mms6</i>	12.7	
	<i>MamR</i>	9.3	
	<i>MamD</i>	30	
Chain assembly	<i>MamJ</i>	48.5	
	<i>MamK</i>	39.2	
	<i>MamY</i>	40.9	

- (2) Uptake of iron ions: The transport and uptake of iron ions cannot be separated from the iron transport system of MTB. For example, in AMB bacteria, the iron delivery system comprises *MamB*, *MamM*, *MamH*, and *MamZ*. After magnetotactic bacteria absorb the iron ions from the surrounding environment, they enter the magnetosome lumen in the form of bound iron or free iron under the action of specific transport proteins (e.g., *MamB* and *MamM*), leading to iron accumulation [28–30].
- (3) Crystal biomineralization: The iron ions entering the magnetosome lumen undergo a series of redox equilibrium reactions under the action of related iron proteins (e.g., *MamE*, *MamP*, *MamT*, and *MamX*) [31], and finally reach the appropriate Fe^{2+}/Fe^{3+} ratio [32]. At the same time, magnetotactic bacteria adjust the physiological and biochemical conditions in the magnetosome vesicles to the most appropriate level (such as high pH value and low redox potential) for crystal nucleation and growth. A series of related proteins regulate the magnetosome crystal shape, number, and size. Some of these proteins (e.g., *MamD*) act as templates to control the spatial configuration of the crystal lattice, and some (e.g., *Mms5* and *Mms6*) control the crystal growth by interacting with the crystal surface [33,34]. In addition, other genes (e.g., *mamS*, *mamR*, *mamN*, *mamF*, and *mms5*) are associated with the size and number of crystals [35].
- (4) Magnetosome chain assembly: The aggregation behavior of magnetosome particles may be subject to internal and external regulatory effects. The external effect is driven by magnetic force, while the internal effect is derived from regulating related proteins. This chain-like form achieves optimal magnetic effects when driven by Earth's magnetic force. Inside MTB, the assembly of magnetosome chains is regulated by the role of associated proteins. Through a series of interactions, magnetosome particles are anchored to a cytoskeletal fibril structure. These proteins act

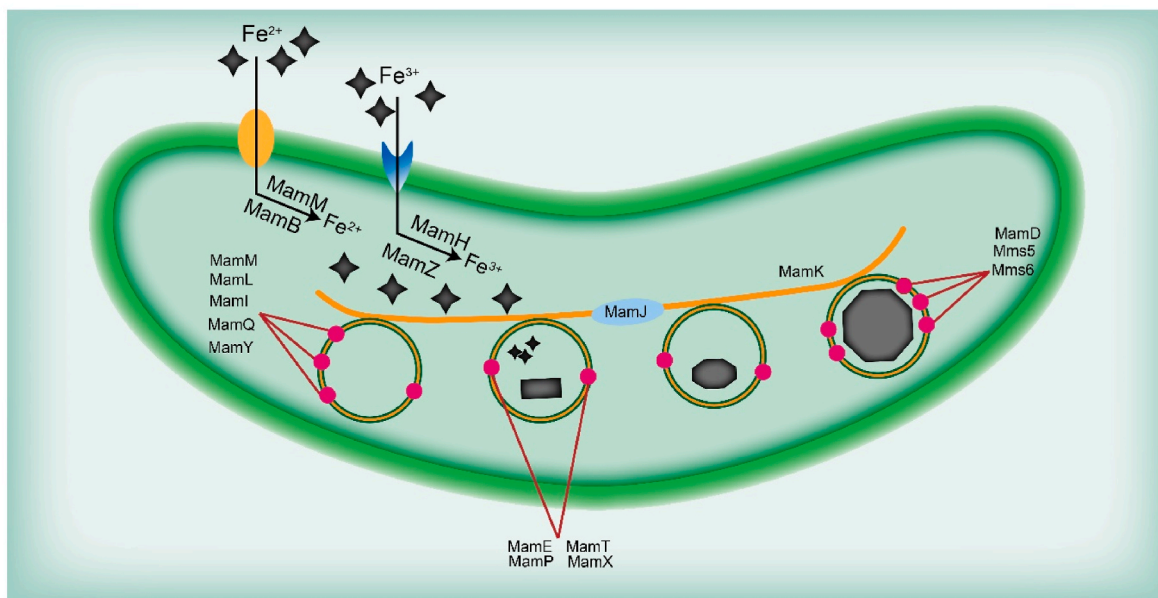


Fig. 2. Illustration showing the mineralization process of magnetotactic bacteria and the role of related proteins in magnetosome biomineralization.

both as anchoring proteins (MamJ) to mediate the attachment of magnetosomes to the cytoskeleton and as actin (MamK) to drive magnetosome movement [36–38]. In addition, Toro-Nahuelpan et al. found a membrane-binding protein MamY in *Magneto-spirillum gryphiswaldense*, which could still promote the formation of discontinuous short chains in the absence of MamK [39]. These results indicated that the molecular mechanism of the chain assembly of magnetosomes remains to need further investigations.

formation is under strict genetic control, resulting in a specific structural morphology and highly ordered single magnetic domain crystals. However, there have been no clinical studies with magnetosomes to date. To better meet the application requirements, necessary modifications must be made before magnetosomes can fulfill broad biomedical applications. The common modification strategies include genetic modification, protein modification, chemical modification, environmental modulation, encapsulation, and mechanical modification (Fig. 3).

4. Methods to modify magnetosomes

Magnetosomes are often mineralized by MTB in which their

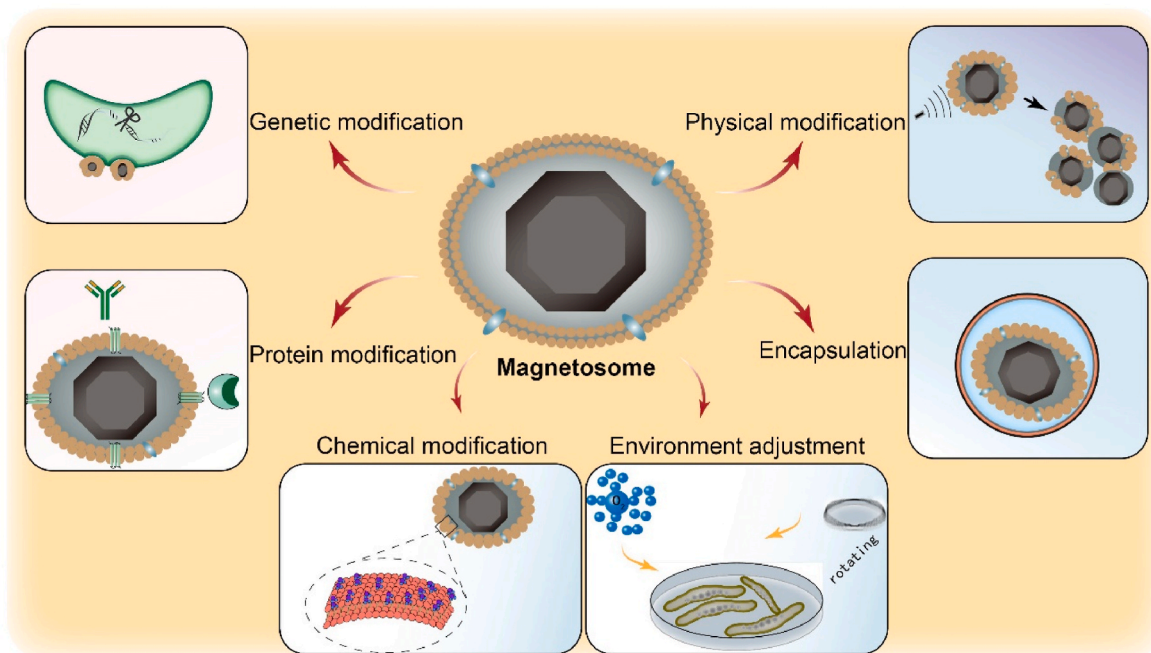


Fig. 3. Illustration of approaches for magnetosome modification, including genetic modification, protein modification, chemical modification, environmental adjustment, encapsulation, and physical modification.

4.1. Genetic modification

Genetic modification is to modify magnetosomes through the gene technology. Currently, genetic manipulation can control the biosynthesis of magnetosomes with pre-designed properties (e.g., protein fusion technology). Protein fusion technology refers to the end-to-end joining of the coding regions of two or more genes to form a gene expression product controlled by the same regulatory regions and sequences [40,41]. Protein fusion technology has been applied in the surface modification of magnetosomes. In a case, Lang et al. constructed fusion proteins using magnetosome membrane genes and green fluorescent protein and eventually obtained green fluorescent protein-tagged magnetosomes by optimizing the growth conditions of MTB [42]. In another case, Mickoleit et al. investigated the potential of *MamA*, *MamG*, and *MamF* as magnetosome anchoring proteins by using a fluorophore (mEGFP) and an enzyme (GusA) as reporter genes [43]. They constructed multifunctional, reusable magnetic composites expressing GusA, glucose oxidase (Gox), mEGFP, and red fluorescent protein (RFP) by fusing mEGFP and GusA with magnetosome membrane proteins through genetic techniques. Meanwhile, the feasibility of

functionalized magnetosomes as reusable multimodal catalysts was demonstrated by introducing the material into hydrogel matrices equipped with mCherry antibodies (Fig. 4A). In addition, magnetosome membrane-associated proteins are encoded and expressed by genomes. Thus, the properties of magnetosome membranes can be modified at the molecular level by using protein fusion techniques. Ginet et al. used the *opd* gene of *Flavobacterium* ATCC 27551 encoding paraoxonase to fuse with the *mamC* gene of the magnetosome membrane to finally obtain magnetosomes with phosphate hydrolase activity, which could be applied as a reusable nano-biocatalyst for the treatment of pesticide effluent [44]. To fine-tune the properties of magnetosomes, Furubayashi et al. designed ribosomal binding sites, minimal constitutive promoters, and large dynamic range induction systems to generate differentially functionalized magnetosomes by affecting the expression of magnetosomal genes [45]. Using the isopropyl β -D-1-thiogalactopyranoside (IPTG) induction system, they anchored super folder green fluorescent protein (sfGFP) to the magnetosome membrane using the MamC protein. They found that cells expressing only sfGFP exhibited diffuse fluorescence, while cells expressing MamC-sfGFP exhibited localized fluorescence that indicated the intracellular location of magnetosomes in the

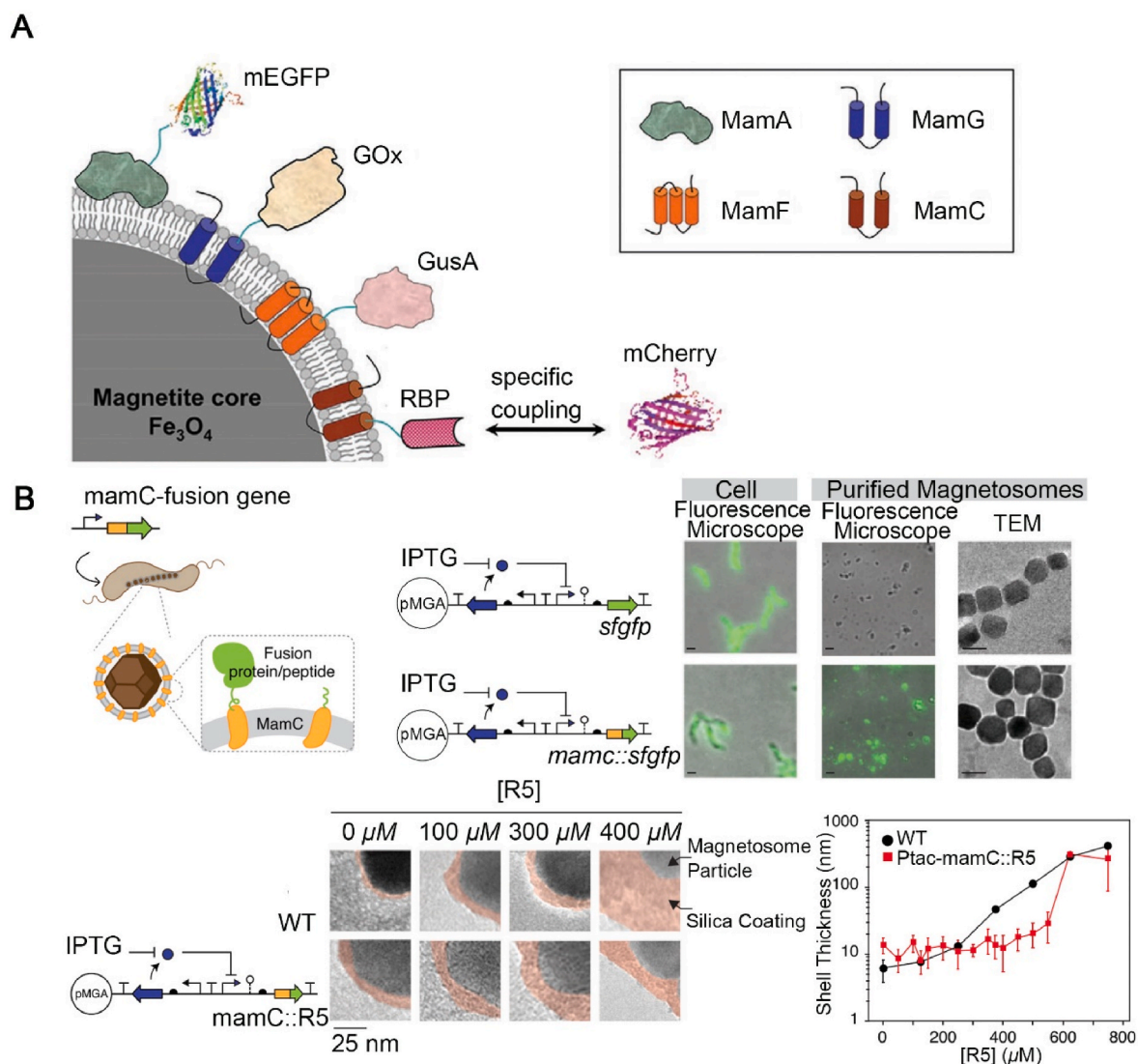


Fig. 4. Genetic modification of magnetosomes. (A) Generation of multifunctional model particles for coupling reactions to mCherry-tagged structures by utilising four different *Mam* proteins as membrane anchors. This approach allowed the surface expression of mEGFP, GusA, Gox, RBP [43]. Copyright 2020, Wiley (B) Using the IPTG inducible system, the expression and localization of sfGFP was compared with the *MamC*::sfGFP fusion. Transmission electron micrographs show silica-coated wild-type and *MamC*::R5 magnetosomes. The silica shell thickness is presented as a function of the R5 peptide concentration [45]. Copyright 2021, Wiley.

cell. They also performed an investigation with the R5 peptide, which nucleates silicic acid. By fusing the R5 peptide with MamC, magnetosomes expressing MamC–R5 appeared surrounded by a 10 nm shell layer without the exogenous R5 peptide. They compared these modified magnetosomes to wild-type magnetosomes in the presence of 300 μ M of the exogenous R5 peptide. In terms of the silica shell layer, the result showed particles gradually increased size with increased concentration of exogenous R5 peptide (Fig. 4B).

4.2. Protein modification

Protein modification is to modify magnetosomes through modifying the proteins on the surfaces of magnetosomes directly. Many methods of nanoparticle-based protein immobilization have been reported, such as electrostatic assembly [46], covalent cross-linking [47,48], and membrane integration [49,50], among others. In contrast, magnetosomes are magnetic nanoparticles presenting a biological core-shell structure that is covered with a lipid bilayer with many active sites. Hence, the structure of magnetosomes also provides a convenient context for protein modification. Pi et al. constructed an antibody-immunomagnetic probe for the enrichment and removal of aflatoxin B₁ (AFB₁) toxin from vegetable oil by attaching AFB₁ polyclonal antibodies to magnetosomes. The enrichment capacity and recovery rate of the antibody-immunomagnetic probe were 115 ng mg⁻¹ and 93.7%, respectively, which were much higher than those of the probe constructed by conventional magnetic nanoparticles [51]. Jacob et al. immobilized lipase onto magnetosomes to improve lipase activity, resulting in the lipase immobilization efficacy on magnetosomes of 88%. Notably, the activity was still high after 30 days of storage at 4 °C compared to free lipase [52].

4.3. Chemical modification

The chemical modification strategy utilizes the abundant primary amine groups on the surface of the magnetosome membrane to modify magnetosomes. Depending on the functional groups introduced into the structure, the commonly used modification methods can be divided into two types [53]. The first step is to couple with amine groups, mainly using cross-linking agents to achieve the coupling between two amine groups. For example, Sun et al. successfully grafted the antitumor drug adriamycin onto a magnetosome membrane with the cross-linking agent glutaraldehyde [54]. The second step is to couple with carboxyl groups; for example, 1-ethyl-3-[3-dimethylamino-propyl] carbodiimide (EDC) can be used to couple carboxyl groups with amine groups. In addition, magnetosomes can be functionalized with the help of certain molecular bridges. Guo et al. used a poly-L-glutamic acid molecular bridge to achieve surface modification of magnetosomes [55]. In an instance, our group has constructed a double cross-linker using genipin and polyglutamic acid, in which genipin could introduce polyglutamic acid to the magnetosomes. The surface modification provided more coupling sites for loading the chemotherapeutic drug cytarabine, effectively increasing drug loading and alleviating the toxic side effects of the drug [56]. The chemical modification of magnetosomes and their applicability will be discussed in the subsequent sections.

4.4. Environmental adjustment

Most MTB in nature require strict growth environments where external factors can affect the crystal size, morphology, and composition of magnetosomes. Usually, different strains produce different crystalline magnetosomes, such as equiaxial or elongated cuboctahedral magnetite magnetosomes by the magnetotactic spiral bacteria, elongated prismatic magnetite magnetosomes by the magnetotactic vibrios and cocci, as well as bullet-shaped face-centered cubic magnetite magnetosomes by the magnetotactic nitrospirillum phylum [57]. In addition, magnetotactic bacteria in the freshwater environment often produce Fe₃O₄-type

magnetosomes. In contrast, magnetotactic bacteria in marine and salt-lake environment accumulate Fe-sulphur-type magnetosomes, mainly composed of Fe₃S₄. Heyen et al. utilised three strains of MTB to evaluate the optimal conditions for magnetosome growth [58]. They found that different strains had different tolerance to oxygen, which greatly affected the iron content of magnetosomes. Li et al. used *Magnetospirillum magneticum* strain AMB-1 under four different growth conditions, such as anaerobic static, aerobic static, aerobic rotating at 80 rpm, and aerobic rotating at 120 rpm, to investigate the effect of the growth environment on magnetosome formation and the magnetic properties of the magnetosomes, from the anaerobic static to aerobic 120-rpm rotating culture. The formed magnetite magnetosomes become more equidimensional, smaller in grain size, and higher in crystal twinning frequency. In addition to the formation of magnetosomes by dynamic incubation was negligible compared to oxygen concentration [59]. The oxygen concentration is critical in forming magnetosomes, in which low oxygen or no oxygen is a necessary condition for synthesizing magnetosomes. The mechanism by which oxygen affects magnetosome synthesis is still being explored. However, the oxygen required for magnetosome biomineralization does not come from the atmosphere but from water. In addition, oxygen can act as a regulatory signal that regulates the expression and activity of specific genes and proteins involved in controlling the grain size, crystal shape, chain arrangement and crystallization of magnetosomes.

4.5. Encapsulation

Magnetosomes are excellent nanocarriers, which are of specific interest for various biomedical applications, including drug delivery. Magnetosomes are often encapsulated into supramolecular networks to improve their pharmacokinetic and pharmacodynamic performances. Commonly used materials to encapsulate magnetosomes include polymers and inorganic materials with good biocompatibility. For example, Borg et al. used the inorganic materials silica or zinc oxide to coat magnetosomes after functionalization to improve their stability [60].

4.6. Physical modification

Natural magnetosomes mostly have a chain-like structure with excellent stability and magnetic responsiveness. However, the magnetosome membrane is not uniformly distributed over the entire chain. Hence, large magnetosome chains can break at a specific location. These short magnetosome chains may exhibit different properties from the large chains. Kobayashi et al. used ultrasound with different pulse periods to destroy the chain of magnetosomes, and then used a magnetometer to measure the magnetic properties of the treated magnetosomes. The results showed that compared with the wild-type magnetosomes, the coercivity of the treated magnetosomes decreased, which might be due to the destruction of the linear structure, making the magnetic moment easier to reverse. [61]. Molcan et al. investigated the magnetic characteristics of short magnetosome chains in direct current (DC) and alternating current (AC) magnetic fields. They sought to balance the magnetosome chain properties with their geometries [62]. They performed ultrasonic treatment on the magnetosomes at a power of 20 kHz and 120 W to shorten the chain length of magnetosomes. They found that the shortened magnetosome chains exhibited different magnetic properties with less energy loss and a reduced specific absorption rate (SAR). The magnetic properties of magnetosomes were balanced with the new stable geometry. In general, using physical means (such as ultrasound) to process the magnetosome chains can change the performance of the magnetosomes. Moreover, these short magnetosome chains possess improved biological permeability toward drug delivery applications.

As discussed, there are various methods for modifying magnetosomes. Genetic modification enables magnetosomes to express the required functional expression, which can meet personalized

requirements. However, due to the need to rely on genetic technology, the operation is oftentimes complicated and requires high requirements. Protein and chemical modifications can directly modify some proteins and chemical drugs on the surface of magnetosomes by virtue of the rich functional groups on the surfaces of the magnetosomes, which are simpler and faster. However, due to the chemical reactions involved, there may be problems such as protein denaturation and low drug loading. Encapsulation and physical modification can improve the performance of magnetosomes through some simple means, but because they are not specific modifications, they can only be used for some simple applications. Environmental adjustment can change the size and even crystal form of magnetosomes. Nevertheless, due to the ongoing research on the mechanism of magnetosomes biomineralization, further understanding is still needed regarding environmental adjustment. In summary, different methods of magnetosomes modification have their own advantages and disadvantages, and specific application conditions need to be considered when applying them. At the same time, the various modification methods can also be combined to better meet application requirements.

5. Cytotoxicity and biocompatibility of magnetosomes

Magnetic nanoparticles have been applied in a wide range of applications in the biomedical and environmental fields due to their exceptional magnetic properties. However, chemically synthesized magnetic nanoparticles are usually modified with chemical reagents (surfactants) to address their toxicity for biomedical applications. In contrast, magnetosomes, as natural magnetic nanoparticles, are covered with a lipid bilayer, which avoids direct contact between the magnetic core and the organism and possesses a negative surface charge preventing the aggregation of magnetosomes. Thus, these hybrid structures of magnetosomes show good biocompatibility, requiring no extensive modifications. Recently, the cytotoxicity and biocompatibility of magnetosomes and chemically synthesized magnetic nanoparticles (ferroferrous oxide nanoparticles) have been evaluated [63]. There are three main methods to assess the cytotoxicity and biocompatibility of magnetosomes (Fig. 5) [64]. The preliminary confirmation is often done

with the methylthiazolyl-diphenyl-tetrazolium bromide (MTT) method in cells *in vitro*. Further, the acute toxicity test at different doses of magnetosomes is performed in mice. Finally, immunotoxicity tests are systematically performed to assess the cytotoxicity and biocompatibility of magnetosomes. However, it should be noted that the tests are not limited to the notified methods [65]. For example, Yan et al. used MTT, hemolysis, and micronucleus assays to evaluate the *in vitro* cytotoxicity, haematotoxicity, and genotoxicity of magnetosomes, respectively, to evaluate the potential of magnetosomes for biomedical applications [66].

Ragulaman et al. compared the cytotoxicity and ecotoxicity of magnetosomes and chemically synthesized ferroferrous oxide nanoparticles by using human red blood cells, macrophage cell lines, onion root tips, *Artemia salina*, and zebrafish embryos [67]. They found that magnetosomes showed an acceptable hemolysis rate and posed no potential environmental risk compared with the synthesized ferroferrous oxide nanoparticles. Qi et al. compared the biocompatibility of magnetosomes and synthetic ferroferrous oxide nanoparticles in human retinal pigment epithelium (ARPE-19) cells to assess cytotoxicity and genotoxicity for the treatment of ophthalmic diseases [68]. They found that magnetosomes were much lesser toxic than synthetic magnetic nanoparticles. Mickoleit et al. evaluated the biocompatibility of magnetosomes using different cancer cell lines and more sensitive primary cells by exploring the cellular activity and death events in the course of magnetosome treatment as well as potential effects on proliferation. The results demonstrated that magnetosomes slightly affected cell proliferation, indicating their suitability in the biomedical field [69]. In another instance, Nan and colleagues evaluated the biocompatibility of magnetosomes extracted from MSR-1. They performed comprehensive *in vivo* and *in vitro* analyses of magnetosomes, including cytotoxicity, mouse body weight measurements, blood tests, organ coefficients, inflammation and hemocompatibility studies. Moreover, the authors demonstrated that magnetosomes showed no signs of cell membrane damage and cell cycle arrest until the concentration was approximately 40 times the clinical dosage, indicating the excellent biocompatibility of magnetosomes [70]. These findings suggest that magnetosomes are biocompatible and have good potential for biomedical and biotechnological applications.

In conclusion, since magnetosomes are derived from bacteria, endotoxin may pose a problem for future use in humans. Thus, the magnetosome-based studies remain at the preclinical stage, requiring comprehensive, biocompatibility and toxicity evaluations for their translation to clinics.

6. Biomedical imaging

Biomedical imaging primarily includes nuclear magnetic resonance and optical-based techniques. The ideal non-invasive imaging platform should exhibit high sensitivity, strong tissue contrast, and exceptional spatial and temporal resolutions. Overall, magnetosomes have excellent properties, showing great potential in MRI and magnetic particle imaging (MPI) applications. Compared with ordinary iron oxide nanoparticles, magnetosomes, as a unique magnetic nanoparticle, offers the advantage of facilitating multifunctional imaging by modifying their membranes.

6.1. Magnetic resonance imaging

MRI, an imaging technique based on the principle of nuclear magnetic resonance, presents a high soft tissue contrast and has been widely considered a reliable diagnostic method. The magnetic resonance signal generated by the object is position dependent [71]. The spatial position of each resonance frequency can be obtained using the Fourier transform analysis. Then, the image of the object in three-dimensional (3D) space can be constructed. MRI has many advantages over traditional imaging techniques, such as high resolution, safety, and multi-directional and

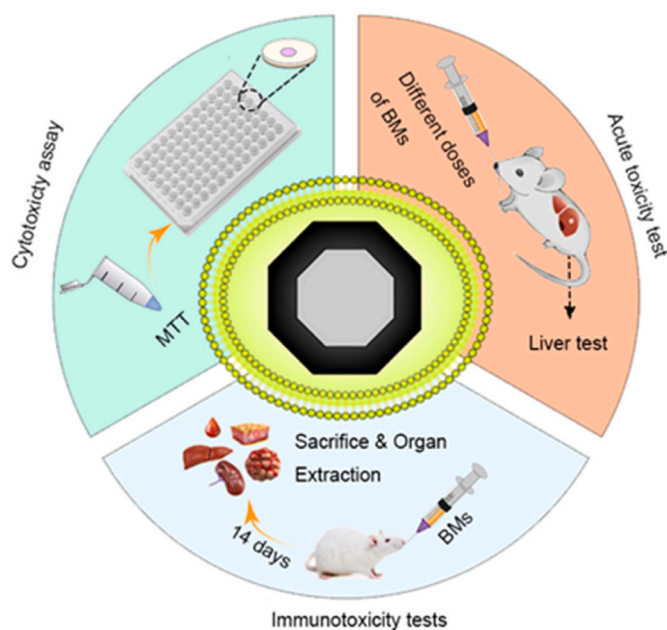


Fig. 5. Schematic illustration of evaluation method for biocompatibility and cytotoxicity of bacterial magnetosomes (BMs), including the methylthiazolyl-diphenyl-tetrazolium bromide (MTT) assay for cytotoxicity and acute toxicity and immunotoxicity tests.

multi-parameter imaging, among others. Therefore, MRI offers become one of the most important imaging tools in the biomedical field.

In addition to proton density, the factors affecting image contrast in MRI are also related to relaxation time. It is essential to determine the relaxation time difference between normal and diseased tissues. Therefore, MRI contrast agents are often used in practical applications to improve imaging noise ratio. MRI contrast agents can be divided into extracellular fluid, blood pool, and specific drugs (Fig. 6A) [72]. The extracellular fluid class is mainly distributed in the extracellular space and is usually used to detect arterial abnormalities and abnormal tissue endothelium. The blood pool class is mainly used to improve the contrast of arterial and venous imaging. Finally, other specific drugs comprise reagents that can target specific organs. Iron oxide nanoparticles as contrast agents have attracted attention in MRI due to their unique magnetic properties and good biocompatibility. Iron oxide nanoparticles (including magnetosomes) for extracellular fluid, can shorten the T2 relaxation time as transverse relaxation contrast agents, enhancing the magnetic resonance signal and darkening the image [73]. It has been shown that the structural parameters of magnetic nanoparticles, including the size, shape, crystal structure, and surface modifications, could affect the performance of MRI contrast agents [74]. In contrast, bacterial magnetosomes have strictly controlled morphologies

and crystalline shapes, mostly arranged in chains. These bacterial magnetosomes possess many advantages (high T2 transverse relaxation rate) over chemically synthesized magnetic nanoparticles in MRI (Fig. 6B). Hu et al. investigated the potential of magnetosomes and chemically synthesized magnetic nanoparticles for magnetic resonance relaxation enhancement [75]. They found that the signal attenuation of magnetosomes was more pronounced than that of chemically synthesized magnetic nanoparticles at the same concentration (Fig. 6C), attributing to the larger aggregate size and stronger ferromagnetism of magnetosomes. Zhang et al. prepared a targeted MRI contrast agent using magnetosomes, which could target tumors that overexpress human epidermal growth factor receptor 2 (HER2) [76]. They used *BALB/c* mice carrying a single SK-BR-3 tumor and a double tumor containing MDA-MB-468 and SK-BR-3 to evaluate the effect of the contrast agent on MRI sensitivity. The prepared magnetosome-based targeted MRI contrast agent accumulated more in the tumor and greatly enhanced the sensitivity of T2 MRI (Fig. 6D).

Overall, magnetosomes have shown promising prospects for MRI application. Several multifunctional MRI contrast agents based on magnetosomes have been developed for real-time monitoring of tumor therapy. It is believed that magnetosomes can be used in clinical practice in the future with further deepening of relevant research.

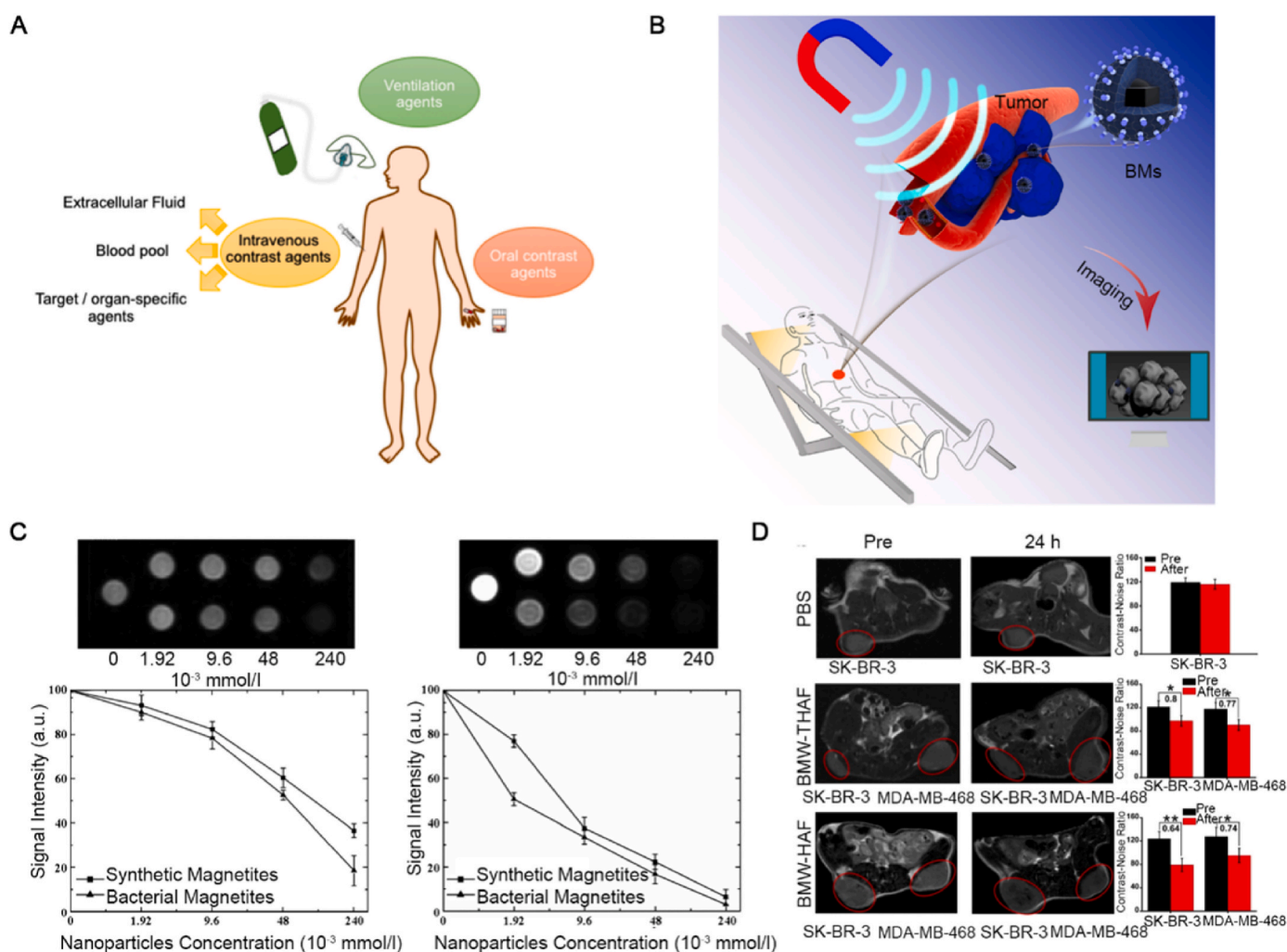


Fig. 6. Application of magnetosomes in MRI. (A) Route of administration of MRI contrast agents [72]. Copyright 2018, American Chemical Society (B) Schematic illustration of bacterial magnetosomes (BMs) used as contrast agents for MRI. (C) T1 and T2 weighted images of several nanoparticle concentrations [75]. Copyright 2010, Institute of Electrical and Electronics Engineers (D) BMW-HAF and BMW-THAF as contrast agents for enhancing MRI [76]. Abbreviations: BMW-HAF, magnetosome with the MamC-HAF protein; BMW-THAF, MamC-THAF-decorated magnetosome; SK-BR-3 and MDA-MB-468, human breast cancer cell lines. Copyright 2018, American Chemical Society.

6.2. Magnetic particle imaging

MPI is an emerging molecular imaging technique based on tracers (superparamagnetic nanoparticles) that bridges the gap between conventional analytical techniques. MPI is based on the Langevin theory of paramagnetism nonlinear magnetization curve, unlike MRI, which uses a static gradient magnetic field (low field strength). With the advantages of linear quantification, positive contrast, no ionizing radiation, no penetration depth limitation, and no biological background signal, MPI has made significant progress in multimodal imaging, cell tracking [77–79], inflammation tracking, drug delivery [80,81], blood pool visualization [82], and tumor detection [83].

Tay et al. used superparamagnetic iron oxide nanoparticles as a tracer to achieve precise magnetothermal therapy for tumors under the guidance of MPI, in which the superparamagnetic iron oxide nanoparticles could be used as tracers for MPI as well as reagents for magnetothermal tumor therapy [84]. This dual function overcame the damage to normal tissues in the surface coil method by using MPI and magnetothermal therapy, allowing the treatment of deep tumors (Fig. 7A). Song et al. used superparamagnetic iron oxide nanoparticles (ferroferric oxide nanoparticles) as a nanopatform for multimodal imaging [85]. They produced whole-body 3D dynamic magnetic particle images of mice (Fig. 7B), showing a slower uptake rate in the spleen and liver compared with VivoTrax (a type of nano magnetic particle). These findings indicated that the prepared superparamagnetic iron oxide nanopatform possessed prolonged circulation time *in vivo* and could achieve long-term and high-contrast MPI imaging. As natural superparamagnetic nanoparticles, magnetosomes possess higher purity, better dispersion, and fewer defects than chemically synthesized magnetic nanoparticles. Therefore, magnetosomes serve as efficient tracers for MPI. Kraupner et al. investigated the potential of

magnetosomes (an average particle size of 36.5 nm) as MPI tracers for studying their structure and magnetic properties [86]. They used a magnetic particle spectrometer system to test the magnetic particle spectrum (MPS) of magnetosomes in a driving field with an amplitude of 10 mT and a frequency of $f_0 = 25$ kHz. The results showed that the MPS performance of all magnetosomes exceeded Resovist, showing the great potential of MPI research.

6.3. Fluorescence imaging

Fluorescence imaging is an optical imaging technique that enables visualizing the distribution of individual molecular substances using the fluorescence emitted by the object examined. Currently, there is an urgent need for precise visualization to determine the diagnosis and treatment of complex diseases, such as cancer, in which traditional computed tomography (CT) and MRI do not allow precise and real-time visualization. Due to no exposure to ionizing radiation, optical can allow a non-invasive real-time visualization, therefore enabling long, safe, and reproducible *in vivo* tissue monitoring [87–90].

Fluorescence imaging based on fluorescent probes is an emerging imaging technique that can selectively detect fluorescently labeled substances in complex mixtures. It has received widespread attention because the high sensitivity and spatial resolution of fluorescence enable fluorescence microscopy to break through the resolution limits of conventional optical microscopy [91]. However, small-molecule fluorescent probes usually lack stability, resulting in rapid quenching in the physiological fluids. To address this limitation, fluorescent probes are required to be encapsulated in the supramolecular carriers. As an excellent magnetic nanocarrier, compared with chemically synthesized magnetic nanoparticles, magnetosomes have the advantages of easy modification and good dispersion, making them the favorable candidate

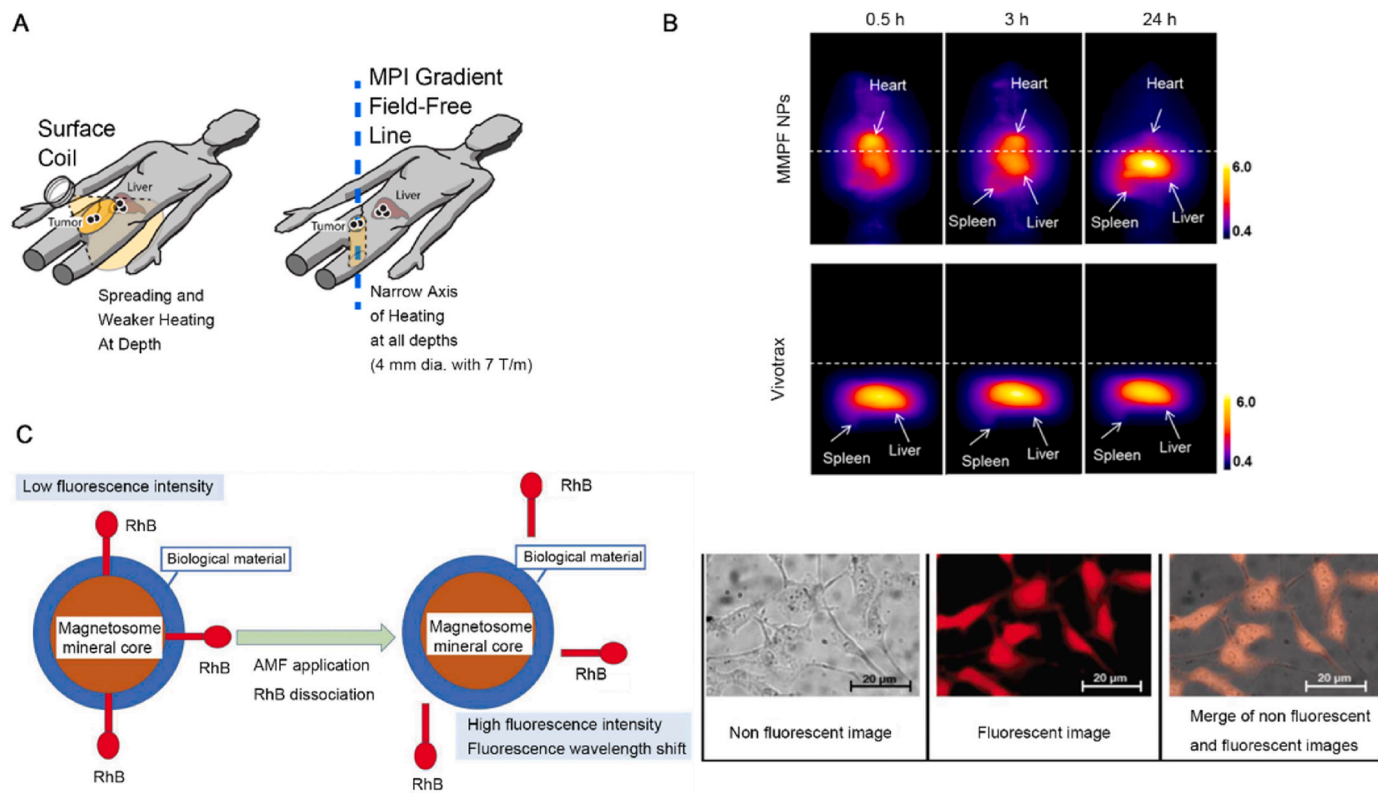


Fig. 7. Application of magnetosomes in MPI and fluorescence imaging. (A) Illustration of MPI-localised heating in the tumor while sparing the liver [84]. Copyright 2018, American Chemical Society (B) Whole-body dynamic 3D MPI images of mice injected with MPI, MRI, photoacoustic, fluorescent nanoparticles (MMPF NPs) and VivoTrax at various time points [85]. Copyright 2019, American Chemical Society (C) Left: illustration showing the operating mechanism of the therapeutic agent (MCR400) probe. Right: micrographs of MCR400 incubated with cancer cells [92]. Copyright 2018, Royal Society of Chemistry.

material for stabilizing fluorescent probes. Alphan ery et al. introduced rhodamine B into the medium of MTB and eventually obtained a fluorescent magnetosome [92]. When exposed to an alternating magnetic field (AMF), rhodamine B dissociated from the magnetosomes and its fluorescence was significantly enhanced (Fig. 7C, left). The microscopic observations of magnetosomes cultured with cancer cells revealed the successful internalization of fluorescent magnetosomes with retained fluorescence (Fig. 7C, right).

Fluorescence imaging has become one of the most important real-time imaging techniques. However, it suffers from several limitations, such as the attenuation and scattering of light, as well as the interference of endogenous fluorescence in living organisms. The development of multimodal fluorescence imaging probes could overcome the shortcomings when using fluorescence imaging techniques alone and improve imaging accuracy and sensitivity. In recent years, fluorescence emission in the near-infrared region has garnered the attention of researchers due to its low background tissue absorption and deeper penetration. For example, Faivre et al. coupled magnetosomes and fluorescent dye to perform MRI and near-infrared fluorescence imaging simultaneously [93]. As a magnetic nanomaterial, magnetosomes could serve as enabling multimodal imaging probes.

In this section, we have summarized the applications of magnetosomes in MRI, MPI, and fluorescence imaging. As a magnetic nanomaterial, magnetosomes have shown exceptional performance in biomedical imaging. The principal reason for its applicability in biomedical imaging is that the surface of magnetosomes is rich in primary amine groups, which can easily react with bifunctional radioactive metal chelators to obtain radiolabeled magnetosomes for positron emission tomography (PET) or single photon emission computed tomography (SPECT) imaging. Patrick and coworkers deposited radioactive metal oxides onto the surface of magnetite nanoparticles and obtained radioactively labeled iron oxide nanoparticles [94], demonstrating that magnetic nanoparticles could be used for PET and SPECT imaging. In summary, the great applicability of magnetosomes in biomedical imaging, they can not only enrich the lesion site through active or passive targeting, but also achieve multimodal molecular imaging for diagnosis and treatment.

7. Anticancer therapy

Cancer usually has unique biological, microstructural, and micro-environmental characteristics. In particular, the tumor microenvironment exhibits the following four major characteristics: i) abnormal acidity, ii) low oxygen concentration, iii) higher glutathione concentration in tumor cells than in normal cells, and iv) elevated hydrogen peroxide [95]. The conventional approaches for cancer treatment include surgery, chemotherapy, and radiotherapy, all of which have limitations, such as being very prone to severe toxic effects on normal cells and tissues due to non-specific treatment. Therefore, it is critical to developing novel cancer treatment methods.

Owing to the small size and large specific surface area of nanoparticles [96], various nanoplatforms have been developed to explore cancer therapy. Magnetosomes have great potential in cancer therapy because of their excellent monodispersity, stability, and biocompatibility. The following sections highlight the recent advances in magnetosomes in cancer therapy, including magnetically induced hyperthermia, magnetically induced photothermal therapy (PTT), and magnetically induced immunotherapy.

7.1. Tumor-targeted drug delivery

Tumor chemotherapy uses highly cytotoxic chemicals that can induce apoptosis or necrosis in tumor cells. The greatest obstacle of chemotherapy is the non-specific damage of the chemotherapeutic agent to normal cells, organs, and tissues. Thus, delivery of the chemotherapeutic agent is a critical issue in chemotherapy. Nanotechnology

provides a novel strategy for anticancer drug delivery [97]. In this context, magnetosome-based chemotherapy has been developed to advance tumor chemotherapy in recent years.

7.1.1. Tumor-targeting strategy

The major challenge of traditional chemotherapeutic drugs lies in the failure to differentiate normal and tumor cells limiting their practical applicability. However, nanotechnology solves this limitation by targeting the tumor cells through active- and passive-based targeting approaches. Due to their large surface area and many surface or internal defects, the highly reactive and active nanoparticle-based tumor-targeting strategies have received significant attention [98]. Researchers have synthesized nanoparticle carriers capable of targeting tumor sites by modifying nanoparticles. For example, Li et al. enhanced the targeting ability of nanoparticles by coating them with cancer cell membranes, enabling immune escape and isotype targeting [99].

As a natural magnetic nanoparticle with surface modifiability, stability, and biocompatibility, magnetosomes have been applied as enabling tumor-targeting carriers. The strategies adopted to modify magnetosomes can be divided into chemical modification targeting and magnetic targeting (Fig. 8A). Unlike chemically synthesized iron oxide nanoparticles, the surface of magnetosomes is covered with a phospholipid bilayer, which has many reactive functional groups, such as primary amines. Using these reactive groups, magnetosomes can be conjugated with specific targeting molecules through chemical reactions. On the other hand, magnetosomes, as magnetic nanoparticles, offer excellent magnetic responsiveness, aggregating at the tumor sites under the intervention of external magnetic fields. In a case, Zhang et al. used genetic techniques and low-frequency ultrasound to obtain magnetosomes with human epidermal growth factor antibodies anchored to MamC on the surface of the magnetosome membrane (Fig. 8B) [100]. In another case, Wang et al. investigated the magnetic targeting ability of magnetosomes by generating a high-gradient magnetic field in a localized area by using a self-built C-type bipolar permanent magnet (Fig. 8C) [101]. In a tumor-bearing mouse model, the magnetic targeting-induced magnetosomes showed a 40% increase in tumor retention. Sangnier et al. developed a magnetosome targeting integral proteins (Fig. 8D) [102]. They synthesized targeted magnetosomes by translational fusion of the arginine-glycine-aspartic acid (RGD) peptide with the magnetosome protein MamC, resulting in the high affinity and cellular uptake by PC3 prostate cancer cells. In the subsequent photothermal experiments, the magnetosomes were also able to effectively inhibit the proliferation of cancer cells.

7.1.2. Drug-loading strategy

Magnetosomes offer excellent potential as drug carriers due to abundant primary amine groups on the magnetosome membrane, in which the chemotherapeutics with suitable functionalities are conjugated to the surface amine groups. In addition, a common strategy involves encapsulating small molecule drugs by using polymers (such as poly(lactic-co-glycolic acid) [PLGA]). The polymers encapsulated with drugs could be attached to magnetosomes, improving the loading efficiency and stability of drugs. Alternatively, chemical drugs with amine groups could be coupled directly to magnetosomes by cross-linking agents (Fig. 9A) [103]. Raguraman et al. explored the loading efficiency of the antitumor drug paclitaxel using glutaraldehyde and 3-aminopropyltriethoxysilane (APTES) functionalization methods, resulting in the resultant drug loading rates of 79.753% and 87.874%, respectively. Further, they evaluated the effectiveness of both methods in terms of drug release and subsequent therapeutic effects (Fig. 9B) [104]. Our group has developed a novel nanocarrier based on bacterial magnetosomes [105] using polyethyleneimine (PEI) as a cross-linking agent to conjugate the antitumor drug doxorubicin (DOX) through hydrazone bonding (DOX loading rate of 57.7%) and small-interfering RNA (siRNA). In addition, we prepared a magnetosome drug loading system [106], choosing genipin and poly-L-glutamic acid as double

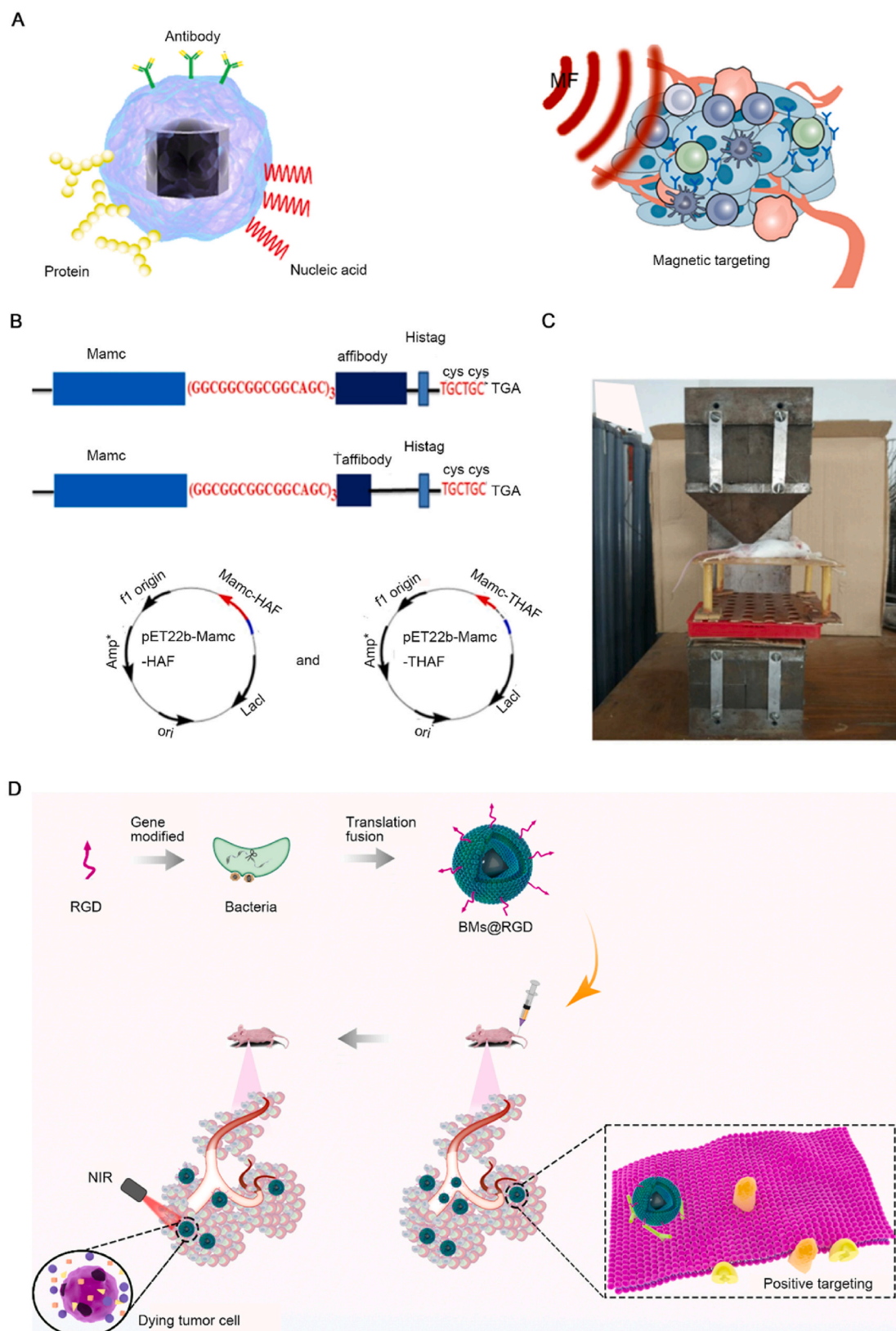
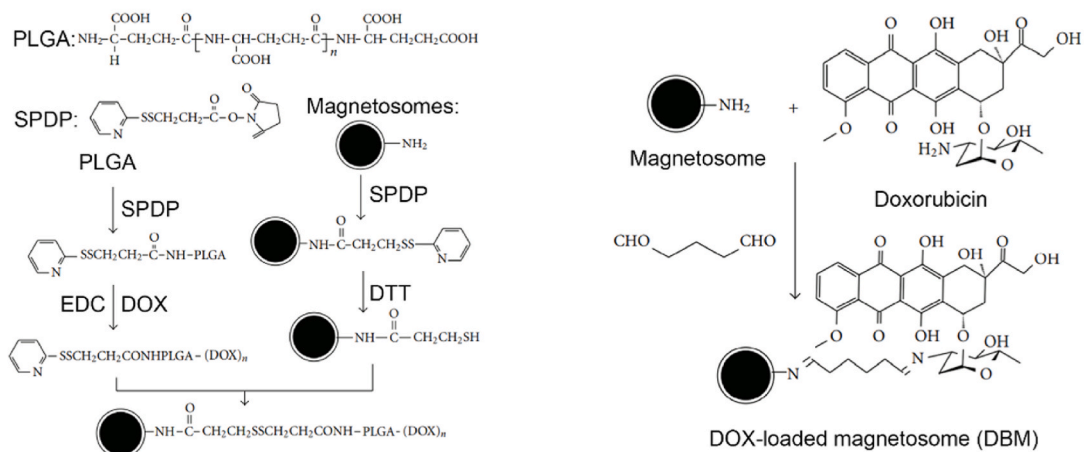
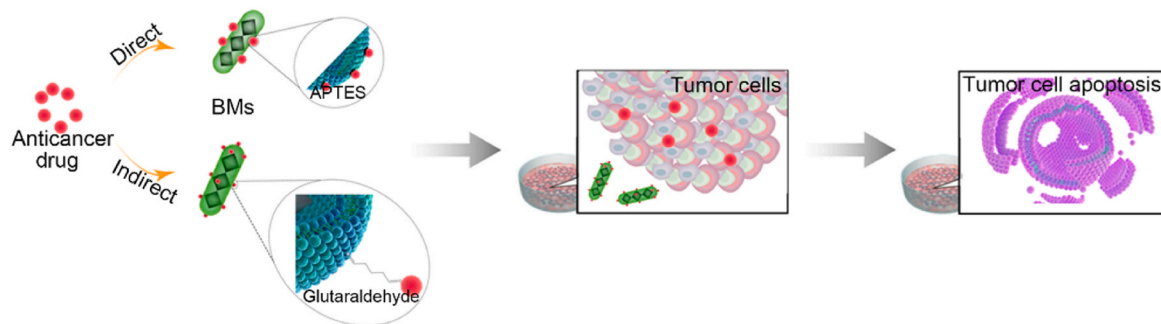


Fig. 8. Targeted modification strategy of magnetosomes. (A) Two targeted modification strategies of bacterial magnetosomes (BMs). (B) Plasmid construction and heterologous expression of *MamC*-HAF and *MamC*-THAF proteins [99]. Copyright 2019, Elsevier (C) Picture of a magnetic targeting experiment [100]. Copyright 2018, American Chemical Society (D) Scheme of RGD peptide-targeted tumor photothermal therapy.

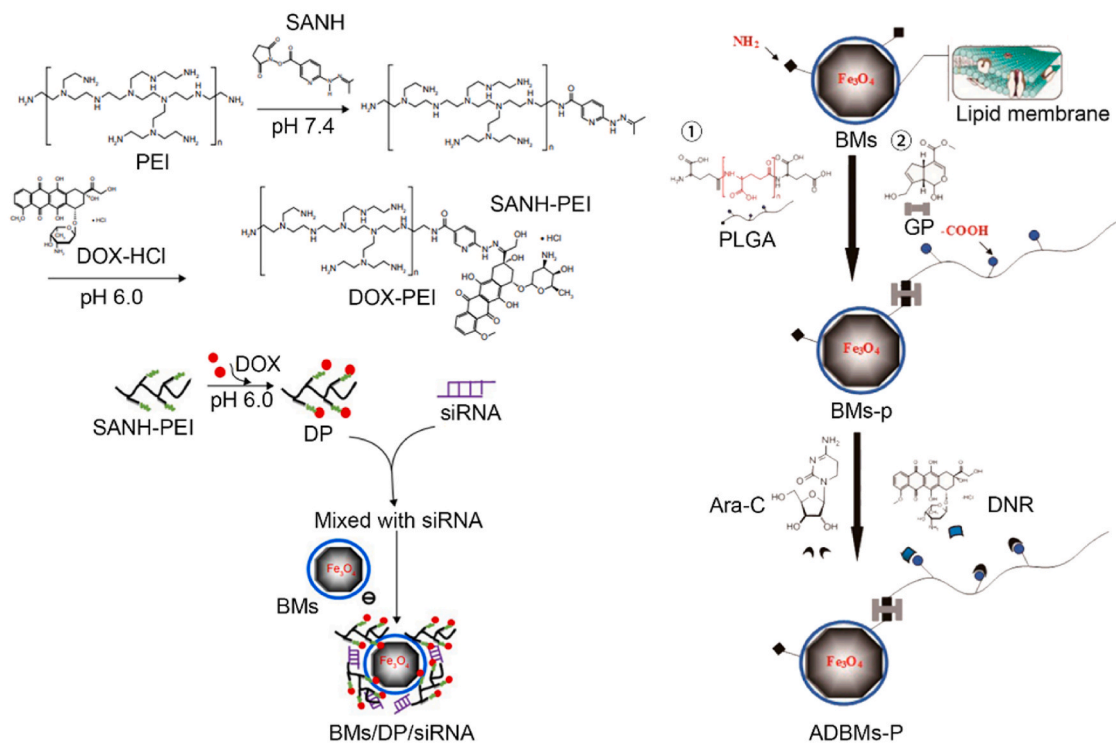
A



B



C



(caption on next page)

Fig. 9. Construction of drug-loading magnetosome carriers. (A) Schematic diagram using PLGA as a bridge to link doxorubicin (DOX) with bacterial magnetosomes (BMs) and preparing DOX-loaded magnetosomes (DBMs) with glutaraldehyde [102]. Abbreviations: SPDP, *N*-succinimidyl 3-[2-pyridyldithio] propionate; DTT, dithiothreitol; EDC, 1-ethyl-3-[3-dimethylamino-propyl] carbodiimide. Copyright 2011, Multidisciplinary Digital Publishing Institute (B) Two ways to drug load BMs for tumor treatment [103]. Abbreviation: APTES, 3-aminopropyltriethoxysilane. (C) Fabrication of BMs/DP/siRNA nanocomplexes and synthesis of Ara-C-DNR-loaded GP-PLGA-modified bacterial magnetosomes (ADBMs-Ps) [104,105]. Abbreviations: DP, DOX-PEI; PEI, polyethyleneimine; SANH, succinimidyl 6-hydrazinonicotinate acetone hydrazine; Ara-c-DNR, arabinoside-daunorubicin; GP-PLGA, genipin-poly-L-glutamic acid. Copyright 2016, Multidisciplinary Digital Publishing Institute and 2018, Elsevier.

cross-linkers, and loaded the anticancer drugs arabinoside (Ara-c) and daunorubicin (DNR) on the surface of magnetosomes (the encapsulation efficiency of Ara-c was 68.4% and the drug loading efficiency was 32.4%, the encapsulation efficiency of DNR was 36.1% and the drug loading efficiency was 17.9%). This approach significantly reduced the non-specific toxicity of the drug combination in tumor therapy (Fig. 9C).

We also found that the drug carrier system showed excellent stability and exhibited continuous long-term drug release. These results have demonstrated the potential application of magnetosomes as drug carriers.

In addition to traditional drug-loaded nanocarriers, stimulus-responsive drug nanocarriers have received increasing attention from

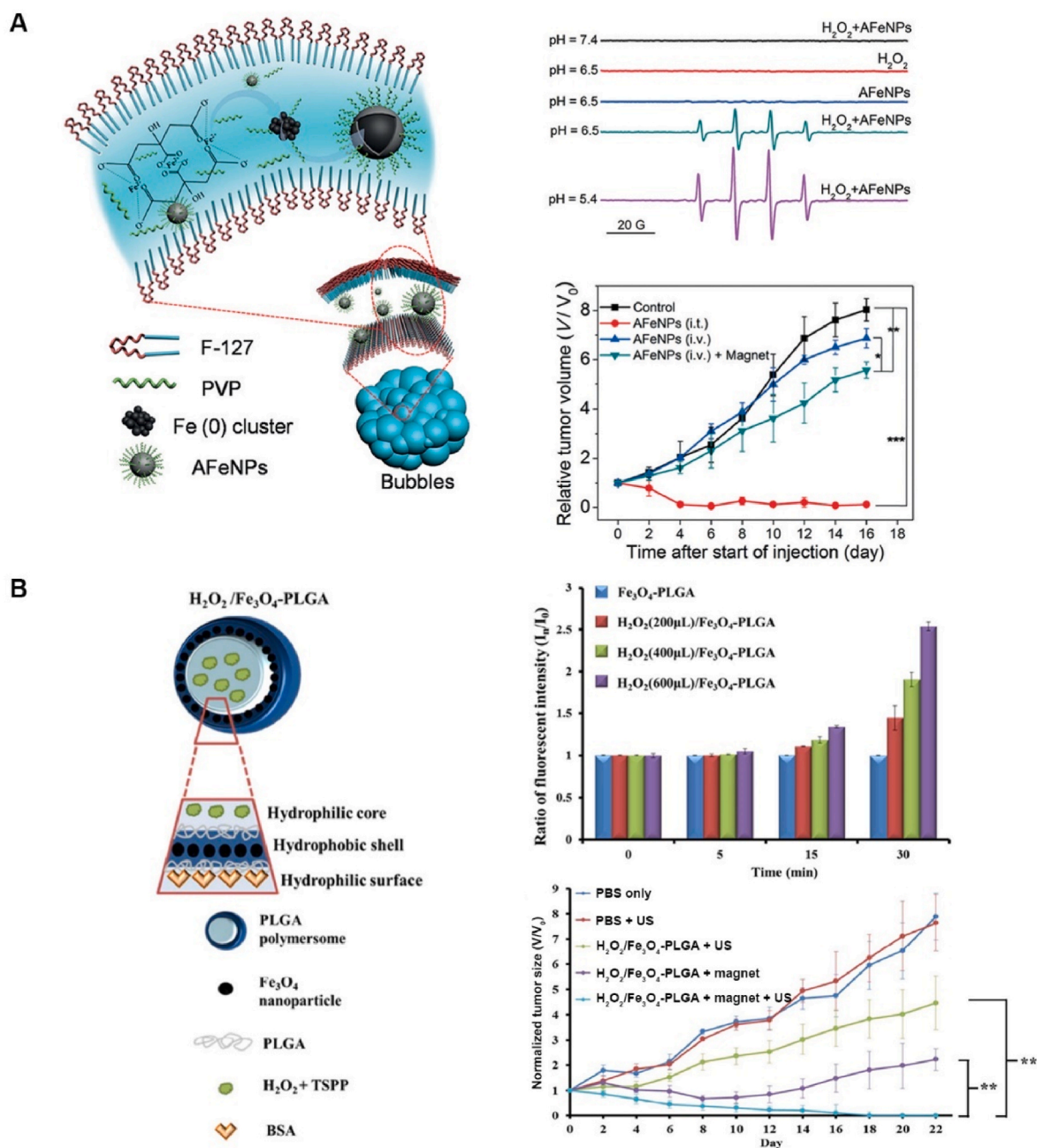


Fig. 10. Application of magnetic nanoparticles in tumor chemodynamic therapy (CDT). (A) Preparation of AFeNPs and treatment effect [107]. Copyright 2016, Wiley (B) Formulated H₂O₂/Fe₃O₄-PLGA polymersomes and antitumor efficacy upon micro-US diagnostic probe (VisualSonics, 40 MHz) irradiation [108]. Copyright 2016, American Chemical Society.

researchers. Targeted to the special microenvironmental characteristics of tumor sites, such drug nanocarriers could minimize the damage of drugs to normal tissues. Therefore, developing such stimulus-responsive magnetosomes as drug nanocarriers is a current research focus.

7.2. Chemodynamic therapy

Chemodynamic therapy (CDT), an emerging nanocatalytic therapy, is considered a tumor-specific treatment with minimal toxic side effects, unlike conventional cancer treatment methods. CDT uses transition metal ions (Fe, Co, Ni, Cu, and Mn) to catalyze overexpressed hydrogen peroxide at the tumor site to produce highly toxic free radicals, such as hydroxyl radicals, through Fenton/Fenton-like reactions. The resultant dreadful free radicals destroy various intracellular biomolecules, such as proteins, lipids, and nucleic acids in tumor cells, causing cell death [107].

Based on the fact that divalent and trivalent iron ions are common catalysts for Fenton/Fenton-like reactions and catalyze them well, several iron-based nanotherapeutic platforms have been developed for CDT of tumors. For example, Bu et al. prepared amorphous iron nanoparticles (AFENPs), which could release Fe^{2+} under weak acidic and excess hydrogen peroxide conditions at the tumor site (Fig. 10A). The catalysis of hydrogen peroxide to produce a large number of hydroxyl radicals could result in the tumor suppression effect *in vivo* demonstrating that AFENPs combined with magnetic targeting could completely inhibit tumor growth [108]. Li et al. fabricated Fe_3O_4 and hydrogen peroxide co-loaded in poly(lactic-co-glycolic acid) (PLGA) vesicles, with hydrophilic hydrogen peroxide in the hydrophilic core and hydrophobic ferric tetroxide nanoparticles in the hydrophobic shell. The design avoided the early reaction of hydrogen peroxide with ferric tetroxide. Further, the collapse of the polymer vesicle structure under the action of external ultrasound and subsequent Fenton reaction between hydrogen peroxide, as well as ferric tetroxide generated excessive hydroxyl radicals, thus inducing tumor cell death and even being able to eradicate tumors [109] (Fig. 10B). Ye et al. constructed a multifunctional magnetic vesicle therapeutic platform using magnetosomes. Magnetosomes could release Fe^{2+} ions under acidic conditions and then generate hydroxyl radicals through the Fenton reaction to induce tumor cell apoptosis [128].

The high tumor-specificity and selectivity of CDT have become one of the main focuses of tumor treatment. However, CDT alone may not achieve the desired therapeutic effect due to its limitation by the high concentration of glutathione and hydrogen peroxide inside the tumor and the strict reaction conditions of the Fenton/Fenton-like reaction (low pH). Thus, the development of a synergistic tumor treatment platform is particularly important. Magnetosomes are expected to be candidates for the combination CDT platform due to their easy modification and the outstanding advantages of the ferric tetroxide core.

7.3. Hyperthermia

Generally, hyperthermia treatment involves heating tumors above the normal physiological tolerance range under external stimulation. Considering the temperature levels, the hyperthermia treatment results in treatment has two effects: i) a high temperature ($>47^\circ\text{C}$) can directly destroy tumors; ii) a mild temperature can improve vascular permeability and change the tumor microenvironment [110]. Furthermore, hyperthermia can also be used in conjunction with other treatments to enhance the effectiveness of tumor treatment. Traditional hyperthermia typically generates heat through external energy (microwave and radio frequency), which usually produces a temperature gradient inside the body. The temperature decreases as the distance from the external energy increases, which is challenging to eradicate deep tumors. Moreover, traditional hyperthermia does not distinguish between tumors and normal surrounding tissues, therefore causing serious side effects on surrounding normal tissues. To solve these problems,

nanoparticle-based hyperthermia with precise targeting effect and a substantial heat generation in the tumor site under external stimulation is required.

Magnetically-induced hyperthermia results in the apoptosis of cells by delivering magnetic nanoparticles to the tumor site and generating heat in response to an applied alternating magnetic field (AMF) (Fig. 11A, left). The frequency of the applied AMF can range from a few kilohertz to 10 MHz, sufficient to penetrate deep enough into the tumor. In recent years, magnetothermal therapy has been applied to several tumor models, such as breast cancer and glioblastoma [111,112]. The main influencing factors in tumor magnetothermal therapy are the strength and frequency of the AMF and the magnetic property of magnetic nanoparticles. In evaluating ferrite nanomaterial-mediated cellular magnetothermal therapy, Zhang et al. demonstrated that cell viability gradually decreased with increased magnetic field amplitude [113]. In magnetothermal therapy, the heat generation mechanisms by magnetic nanoparticles in response to an applied AMF include hysteresis loss and relaxation loss, which are related to the magnetic property of magnetic nanoparticles. Generally, hysteresis loss is observed in multi-domain nanoparticles. When the applied magnetic field changes, the magnetization strength of the nanoparticles themselves lags behind the magnetic field strength, thus generating a loss and converting the energy into heat. Single-domain or superparamagnetic nanoparticles often experience relaxation loss, divided into Néel loss and Brown loss. Néel loss is the loss of the internal magnetic moment of the nanoparticle with the change in the external magnetic field, resulting in a phenomenon from the tilt of the particle spin. Brown loss is related to the free rotation of the particle [114]. Specifically, when the external magnetic field changes, the rotation of the particle lags behind the change of the magnetic field, resulting in the generation of friction with the surrounding liquid (Fig. 11A, right) [115,116]. As a type of superparamagnetic nanoparticle, the heating mechanism of magnetosomes is usually the result of the superposition of Néel loss and Brown loss. However, it should be noted that the resultant effects of these two mechanisms depend on the nanoparticle size. Generally, when magnetosomes gather into magnetosome chains, the contribution of Brown relaxation dominates, while Néel relaxation dominates for single magnetosomes [117,118].

Bacterial magnetosomes have been used for hyperthermia treatment because their iron oxide cores can generate heat under the application of AMF. Synthetic magnetic nanoparticles often suffer from several limitations, such as unstable magnetic characteristics induced by the non-optimized magnetic properties and aggregation-induced toxicity due to their small sizes. To this end, using magnetosomes could substantially avoid such drawbacks of synthetic magnetic nanoparticles. MTB use their internal chains of magnetosomes to sense and respond to external magnetic fields. Accordingly, Gandia et al. investigated the magnetothermal efficacy of MTB in cancer therapy and determined the thermal efficiency of MTB using calorimetry and AC magnetometry [119]. Using human lung A549 cancer cells, they examined the cytotoxicity and thermotherapeutic efficiency of the *Magnetospirillum gryphiswaldense* strain MSR-1. These bacteria could increase the medium temperature to $40\text{--}45^\circ\text{C}$ quickly by applying an external magnetic field with an amplitude of ≥ 300 Oe and a frequency of 300 kHz, demonstrating excellent magnetothermal efficacy (Fig. 11B). Liu et al. compared the magnetothermal effect of magnetosomes with synthesized magnetic nanoparticles and examined cytotoxicity by using human MCF-7 breast cancer cells [63]. Under the same AMF intensity, the magnetosomes showed a better heating effect than synthesized magnetic nanoparticles. In addition, the acute toxicity assessment in mice showed that the lethal dose of magnetosomes was higher than that of chemically synthesized magnetic nanoparticles.

Alphandéry et al. extracted a well-crystallized, chain-like arrangement of magnetosomes with a single magnetic domain structure from the *Genus species* strain AMB-1. They compared the heat production efficiency of intact MTB, magnetosome chains, and individual

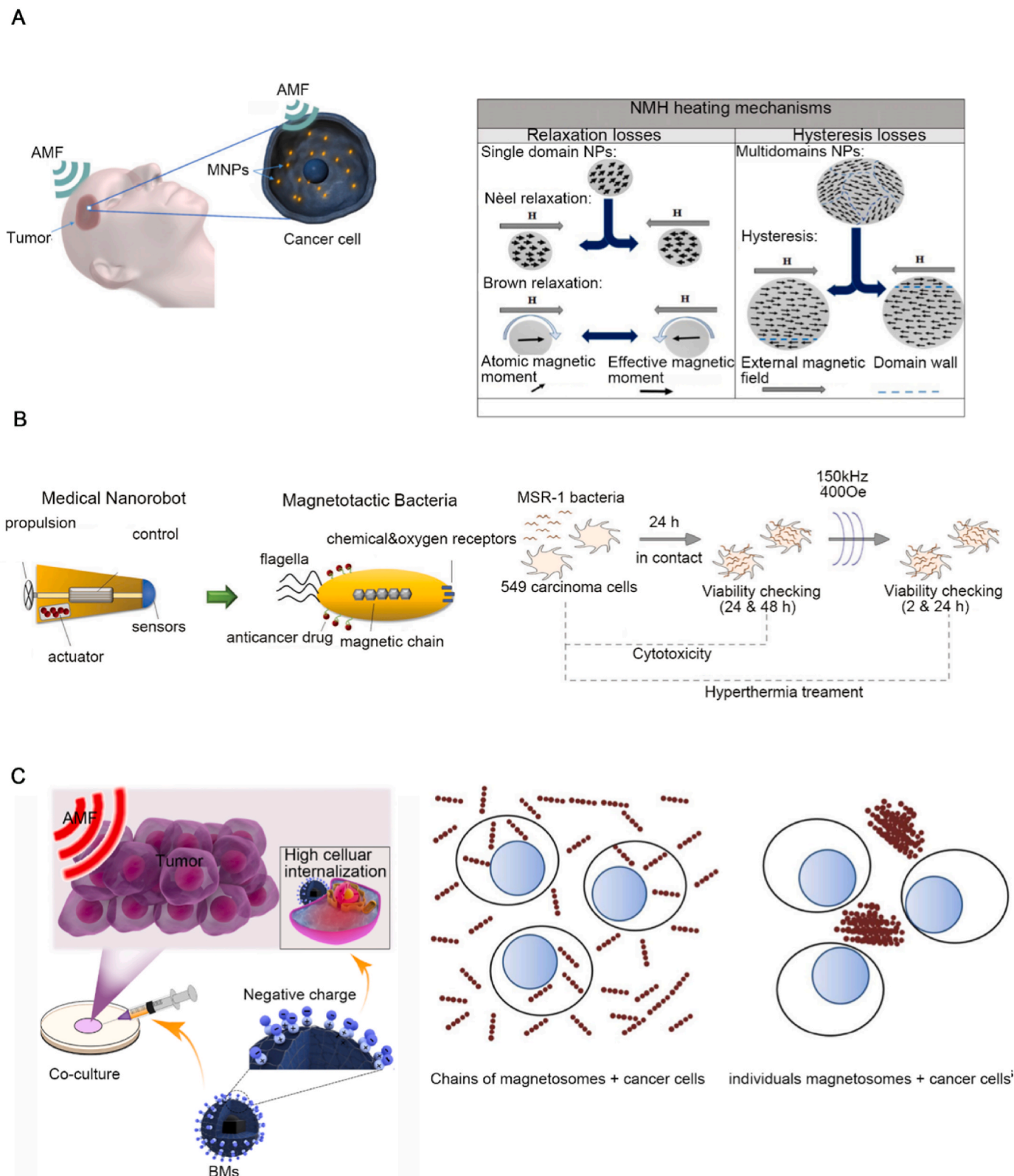


Fig. 11. Application of magnetosomes in magnetic hyperthermia. (A) Magnetic nanoparticles (MNPs) are injected and travel to the tumor. They are then exposed to an AMF to generate heat inside the tumor [114]. Copyright 2016, Elsevier (B) Left: illustration of the necessary characteristics of a medical nanorobot used for cancer treatment. Middle: illustration of a magnetotactic bacterium functionalized with anticancer drugs. Right: schematic diagram for an *in vitro* assay carried out to determine the potential cytotoxic effect of *Magnetospirillum gryphiswaldense* strain MSR-1 and the effect of hyperthermia treatment in human lung carcinoma cells [118]. Copyright 2019, Wiley (C) Illustration of the effect of magnetic heating of bacterial magnetosomes (BMs), the spatial distribution of magnetosomes, and the magnetosome penetration of cancer cells [120]. Copyright 2012, Elsevier.

magnetosome nuclei in an AMF [120]. The SAR of these three magnetic samples was more significant than that reported for smaller superparamagnetic nanoparticles. In addition, the authors investigated the heat production mechanism of three magnetic samples attributing to hysteresis loss for intact MTB and single magnetosome nuclei, and relaxation loss for magnetosome chains. In addition, Alphandéry et al. investigated the efficiency of magnetosome chain aggregates and individual magnetosomes in magnetothermal therapy by co-incubating them with cancer cells and then observing the inhibitory effect of cancer cells after exposing them to an AMF [121]. The magnetosome chain aggregates achieved more efficient heating than individual magnetosomes. This outcome could be attributed to the increased cell membrane permeability with an increase in temperature, making it easier for magnetosome chains to penetrate cancer cells. The negative electrical properties of magnetosome chain surfaces might have also promoted cell internalization. On the contrary, individual magnetosomes could not effectively inhibit cancer cell proliferation, owing to the tendency to aggregate and instability (Fig. 11C).

Magnetosomes are good candidates for magnetothermal therapy under their natural magnetic nanomaterial and reduced toxicity to normal cells. Moreover, there are some new strategies to improve the magnetothermal therapy of magnetosomes. Le Fevre et al. reported a magnetosome wrapped by polylysine (M-PLL), which showed high antitumor efficacy on glioblastoma magnetothermal therapy and maintained the tumor temperature at 43–46 °C for a longer time [122]. PLL wrapping improved magnetosome biocompatible and colloidal stability, which could be the reason for improved photothermal-based therapeutic effects. Mandawala et al. isolated magnetosomes from MSR-1 magnetotactic bacteria, and purified them to remove potentially toxic organic bacterial residues initially. Then, the isolated bacteria were stabilized with poly L-lysine (N-PLL), citric acid (N-CA), oleic acid (N-OA) or carboxymethyl glucan (N-CMG). Further, they tested the antitumor and heating effect of magnetosomes *in vitro* by using GL-261 glioblastoma cells and applying AMF (198 kHz and 34–47 mT). The results showed the destruction rates of tumor cells ranging from 10 ± 3% to 43 ± 3% [123].

7.4. Photothermal therapy

PTT, is another promising antitumor strategy, involves the delivery of the photothermal agent to the tumor site and generates heat under laser irradiation at a specific wavelength (such as near-infrared light) to trigger tumor cell apoptosis [124–126]. The basic principle of photothermal conversion is that light absorbed by a photosensitive material leads to the transfer and transmission of energy, finally emitted in the form of heat through electron radiation leap or other mechanisms. The ideal photothermal agent should be non-toxic or low toxicity and possess excellent biocompatibility. Various nanomaterials have been developed as photothermal agents, including graphene, gold nanostructures, Pd nanosheets, and cobalt dihalide [127]. However, these nanomaterials have a long retention time in the body, thereby causing damage to normal tissues. To this end, the organic-based photothermal agents can be eliminated rapidly from the body. In addition, the most commonly used organic photothermal agents suffer from poor aqueous stability and cause significant toxicity, requiring a suitable nanocarrier to improve their stability.

Peng et al. generated gold nanoparticles *in situ* on magnetosome membranes through a simple seed growth process, constructing a multifunctional magnetosome platform that integrated targeting, imaging, and therapy [128]. The fabricated gold nanoparticles could be used as glucose oxidase to consume glucose at the tumor site for tumor starvation therapy and as a photothermal agent for tumor PTT. The magnetosome component possessed magnetic targeting and MRI abilities. They investigated the therapeutic performance of MSC-Au *in vivo* by using a 4T1 mouse tumor model. After the effect of the magnetic field, MSC-Au gathered at the tumor site, and the temperature of the tumor

increased by more than 17 °C in 1 min after a single laser irradiation (808 nm, 1 W/cm²). After 8 days of treatment, the mouse tumor was eliminated. The multifunctional magnetosome platform showed good photothermal conversion ability, producing a better tumor suppression effect (Fig. 12A).

In 2011, Chen and colleagues first reported that Fe₃O₄ nanomaterials showed photothermal effects (808 nm, 640 mW/cm²) and explored the inhibition effect on bacteria by laser irradiation [129]. Iron oxide nanoparticles have been recognized by the U.S. Food and Drug Administration (FDA) as nanomaterials without potential toxicity [130], endowing them with a more significant advantage in biomedical applications than some other nanoparticles. In contrast, magnetosomes mineralized by MTB have an iron oxide core encapsulated by a lipid bilayer, providing superior biostability and biodistribution properties, making magnetosomes promising photothermal agents. The basic process of magnetosome-based tumor PTT involves the internalization of magnetosomes by the cancer cells and then exposure to near-infrared light (808 nm), generating heat and reactive oxygen species to induce tumor cell apoptosis (Fig. 12B, left). Recently, Sangnier et al. studied the photothermal performance of magnetosomes modified with RGD peptides (magnetosome@RGD) [102]. They compared the photothermal and magnetic hyperthermia efficiency of magnetosome@RGD, demonstrating that the photothermal efficiency of magnetosome@RGD was higher than that of magnetic hyperthermia efficiency *in vivo*. They verified the photothermal effect of magnetosomes *in vivo*, indicating that, after 10 days of photothermal treatment (808 nm, 1.5 W/cm²), magnetosome@RGD could completely inhibit tumor growth (Fig. 12B, right). Therefore, using magnetosomes as combined photothermal and magnetothermal reagents is feasible. Chen et al. investigated magnetosomes for PTT under the guidance of MRI [131]. Transmission electron microscopy revealed that the magnetic nanoparticle core of magnetosomes was covered by a 2-nm-thick biofilm. In addition, high-resolution transmission electron microscopy showed that magnetosomes possessed a single crystal structure with an interlayer distance of 0.26 nm, consistent with the face-centered cubic structure of iron oxide (311) crystalline surface (Fig. 12C, left). These results indicated that the core of magnetosomes is a typical iron oxide nanoparticle, and the subsequent experimental results confirmed that the magnetosomes could be used not only as a photothermal agent for tumor PTT but also as a contrast agent for MRI to guide tumor PTT to monitor distribution (Fig. 12C, right).

Owing to the lipid bilayer on their surface, avoiding the need for secondary modification and enhancing biocompatibility, magnetosomes should have a bright future in tumor PTT. Although some progress has been made for magnetosome-based PTT, some problems still need to be solved. For example, the current tumor PTT mainly uses light sources in the near-infrared region for excitation, which lacks the ability to penetrate deep tumors. In addition, magnetosomes may have endotoxin-related problems and have only been evaluated pre-clinically, and there has been no significant progress in clinical translation.

7.5. Immunotherapy

Immunotherapy utilizes the human body's immune system to fight against tumor cells. Tumor immunotherapy has made tremendous strides that have attracted widespread attention. Various immune cells, such as macrophages and T cells, exist in the tumor microenvironment. Immune cells can recognize cancer cells, especially those that cross the physiological barrier, which places them in a unique position for cancer treatment. While occupying the normal tissues of the body, cancer cells gradually develop a series of camouflages to evade immune system checks. The associated immune cells also express negative regulators, contributing to the formation of the tumor immune microenvironment [132].

Under normal conditions, tumor cells release relevant antigens, which are presented to lymphoid tissues by antigen-presenting cells.

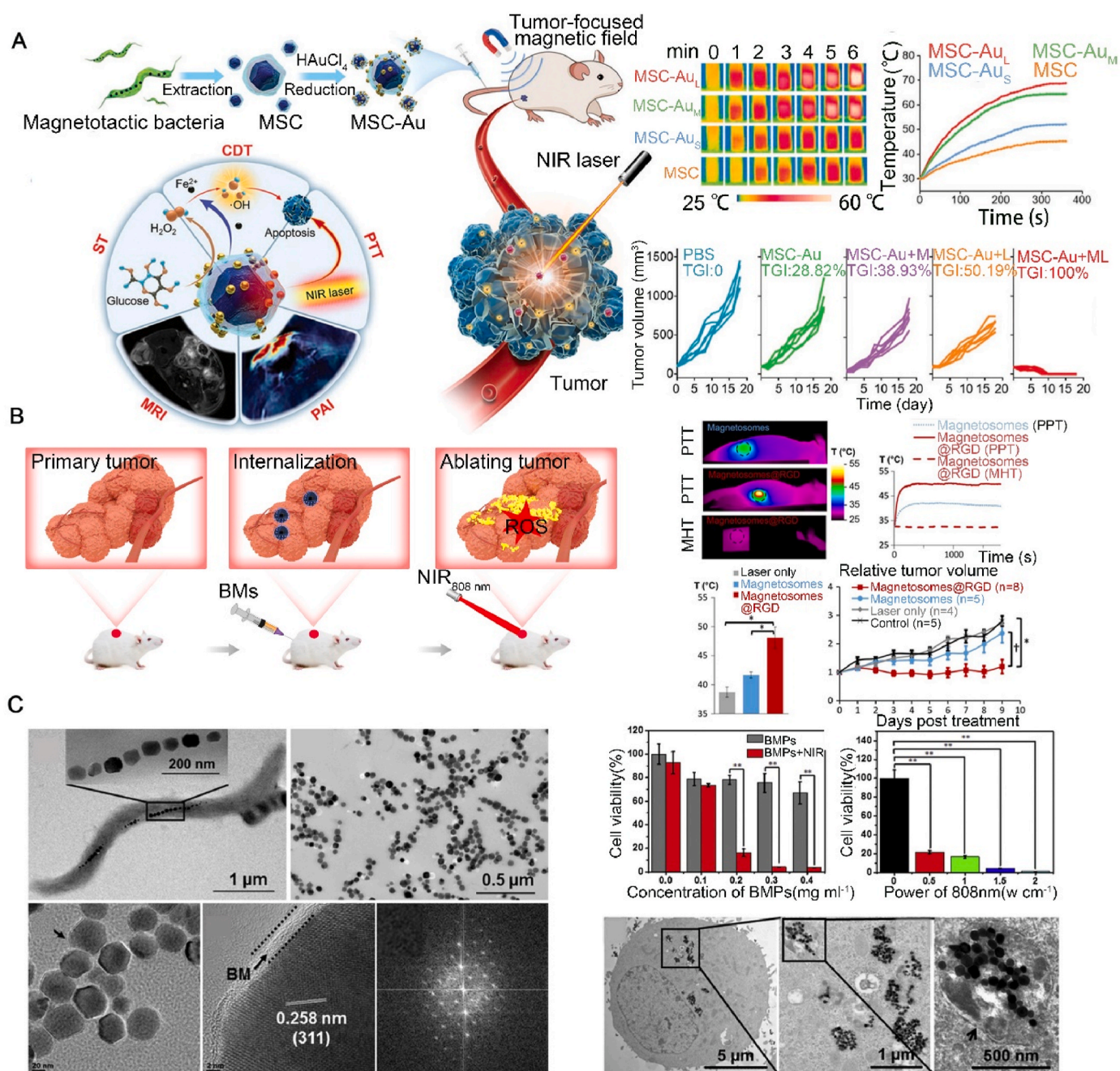


Fig. 12. Application of magnetosomes in photothermal therapy. (A) Schematic of magnetosome chassis (MSC)-Au construction and imaging-guided multimodal therapeutic effects. MSC-Au was constructed by *in situ* growth of Au nanoparticles on the biomembrane of MSCs extracted from *Magnetospirillum magneticum* strain AMB-1. After intravenous injection, MSC-Au efficiently accumulated in tumors because of the tumor-focused magnetic field, which was monitored by photoacoustic imaging (PAI) and MRI. Upon laser irradiation, MSC-Au in tumors provided multiple treatments, including starvation therapy (ST), chemo-dynamic therapy (CDT), and PTT [127]. Copyright 2022, Wiley (B) Illustrations of bacterial magnetosomes (BMs) for photothermal cancer therapy and heating efficiency of magnetosomes [101]. Copyright 2018, Elsevier (C) Transmission electron micrograph of *M. magneticum* strain AMB-1 and bacterial magnetic nanoparticles (BMPs), the results of PTT for HepG2 cells *in vitro*, and intracellular distribution of BMPs [130]. Copyright 2016, Elsevier.

This action activates specific T cells in lymphoid tissues, infiltrating tumors and clearing relevant antigens. In addition, macrophages in the tumor microenvironment can be polarised into the M1 phenotype, expressing inflammatory cytokines and promoting T-cell differentiation to the Th1 type to enhance the immune response (Fig. 13A) [133].

In recent years, researchers have developed bionic magnetosomes based on the structure of native magnetosomes. They have been used to design multifunctional nanoplatforms with unique advantages in tumor immunotherapy. Zhang et al. engineered bionic magnetosomes (Pa-M/Ti-NCs) for ferroptosis and immunomodulatory synergy in cancer

therapy using magnetic iron oxide nanoclusters and leucocyte membranes [134]. Specifically, they anchored programmed cell death protein 1 (PD-1) antibodies and transforming growth factor beta (TGF- β) inhibitors on the leucocyte membranes for immune checkpoint and targeted therapies. The magnetic nanoparticle cores could be used for magnetic targeting by MRI. The iron ions in the nanocore could catalyze the decomposition of hydrogen peroxide and generate hydroxyl radicals in the Fenton-like reaction to induce ferroptosis in tumor cells (Fig. 13B, left). Synergistic inhibition of PD-1 and TGF- β significantly increased the levels of CD4⁺ T cells, CD8⁺ T cells, and macrophages (Fig. 13B, right).

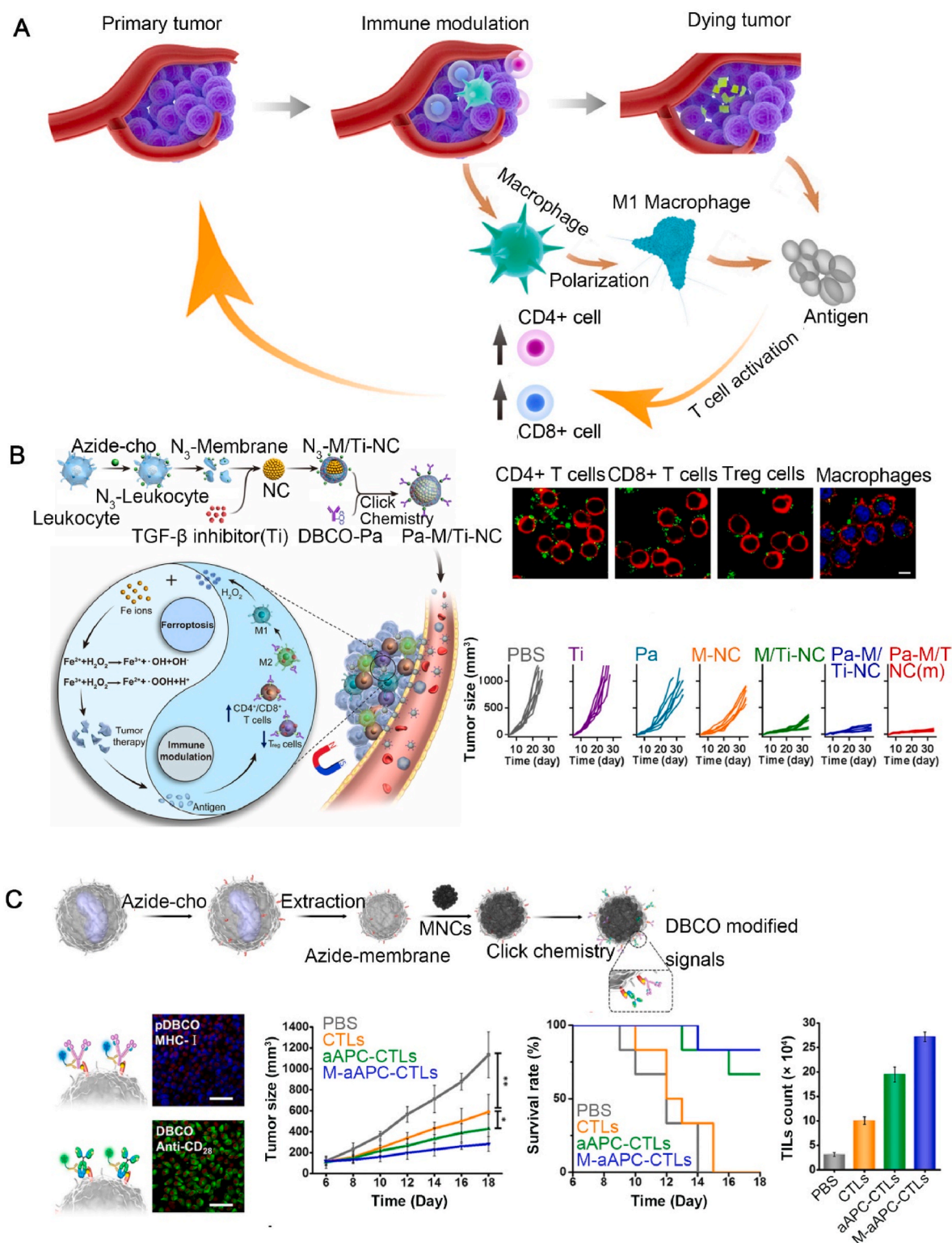


Fig. 13. Application of biomimetic magnetosomes in tumor immunotherapy. (A) Scheme of immunomodulation for tumor treatment. (B) Illustration of a biomimetic magnetosome for ferroptosis/immunomodulation synergism in cancer and tumor immune microenvironment changed by biomimetic magnetosome [133]. Copyright 2019, American Chemical Society (C) Construction of a bionic magnetosome nanoplatform and its application in T cell-based anticancer therapy [134]. Copyright 2017, American Chemical Society.

The antitumor effect *in vivo* showed that Pa-M/Ti-NCs almost completely inhibited tumor growth after applying a magnetic field to the tumor area. Zhang et al. prepared a bionic magnetosome nanoplatform through a superparamagnetic nanoparticle cluster and azide-modified leucocyte membrane fragments [135]. They loaded azide-modified leucocyte

membranes with major histocompatibility complex class I (pMHC-1) and co-stimulatory ligand anti-CD28 (α CD28) by using dibenzocyclooctyne (DBCO) with copper-free click chemistry. The superparamagnetic nanoparticles enabled MRI monitoring by enhancing T2 relaxation properties. Moreover, it could be observed from the

evaluation of the anticancer effect that the bionic magnetosome showed an excellent tumor inhibition effect after applying a magnetic field (Fig. 13C).

There have been numerous developments in tumor immunotherapy,

and its efficacy highly depends on the effective stimulation of specific immune cells. Some key problems remain with active immunotherapy, such as poor and time-consuming stimulation of specific T cells by natural antigen-presenting cells. In addition, these specific T cells rarely

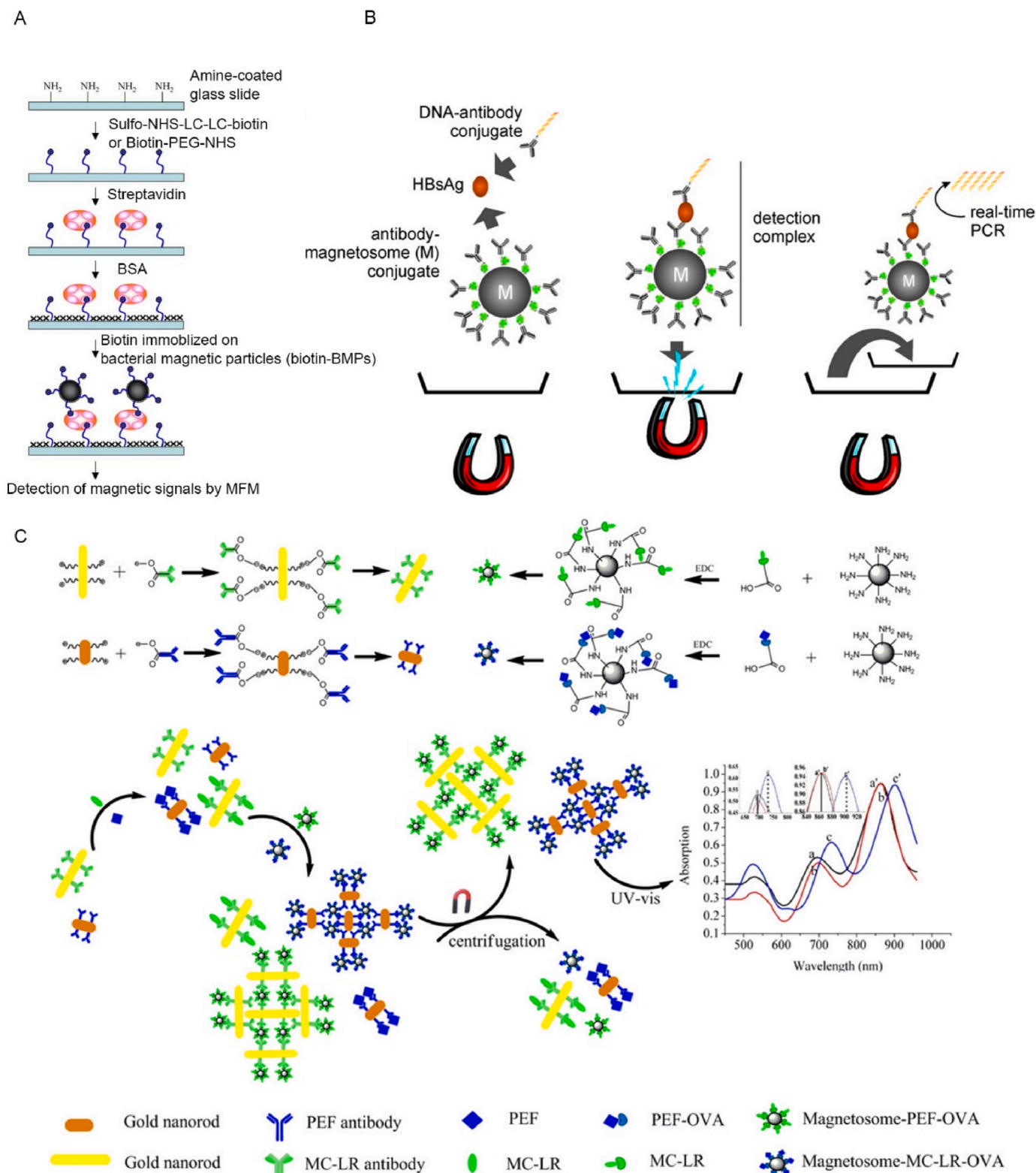


Fig. 14. Application of magnetosomes in biosensors. (A) Procedure of magnetic detection for streptavidin by using biotin-bacterial magnetic particles (BMPs) and magnetic force microscopy (MFM) [136]. Copyright 2005, Elsevier (B) Schematic drawing of the Magneto Immuno-PCR (M-IPCR) [137]. Copyright 2007, Elsevier (C) Schematic illustration of the developed longitudinal surface plasmon resonance assay using the specified gold nanorods probes and magnetosome probes [138]. Copyright 2013, Elsevier.

reach the tumor. The unique properties of magnetosomes may represent a way to address these issues, because magnetosomes and magnetosome-like structured nanoplateforms exploit the magnetic responsiveness of the core of magnetic nanoparticle clusters to deliver relevant immune adjuvants to tumor sites accurately and monitor their distribution *via* MRI. In addition, the biofilms in magnetosomes and magnetosome-like structures could prolong the circulation time and serve as a source of interaction forces to load different types of drugs. In conclusion, magnetosomes and magnetosome-like nanoplateforms are promising strategies in tumor immunotherapy.

8. Biosensor

Biosensor technology is a multidisciplinary analysis technology involving biology, chemistry, physics, and other disciplines. This approach uses immobilized sensitive materials to recognize or sense elements (including enzymes, antibodies, antigens, microorganisms, etc.) and convert the biological reaction information into quantitative digital signals through appropriate conversion. Because of their strong specificity, high speed, and high sensitivity, biosensors have broad application prospects in clinical testing, biomedicine, and environmental monitoring. Accordingly, magnetosomes can be applied as biosensors due to their rich membrane proteins and magnetic response properties.

Magnetosome-mediated biosensors are mainly used to detect target substances by modifying antibodies or antigens and other biological sensing elements on the membrane of magnetosomes. Wu et al. constructed an electrochemical biosensor based on magnetosomes to detect staphylococcal enterotoxin B (SEB) in milk. The SEB antibody functionalized magnetosomes were deposited on the surface of the gold electrode and recorded the change of electrode impedance to detect SEB quantitatively. The detection range was 0.05–5 ng mL⁻¹, and the detection limit was 0.017 ng mL⁻¹ [136]. Amemiya et al. developed a magnetic biosensor for detecting streptavidin using biotin-conjugated magnetosomes. The magnetosomes were used as magnetic markers for magnetic microscope imaging, and magnetic signals could be obtained by magnetic microscope without applying an external electric field (Fig. 14A). The detection limit of streptavidin in this sensor was 1 pg mL⁻¹, which was 100 times higher than the sensitivity of a conventional fluorescence detection system [137]. Acker et al. used magnetic immuno-PCR technology to build an antigen detection biosensor and used the recombinant hepatitis B surface antigen (HBsAg) model for testing (Fig. 14B). After combining the biotinylated magnetosomes with streptavidin, they coupled with the biotinylated HBsAg antibody to form a magnetosomes complex, mainly used for antigen fixation and magnetic enrichment [138]. When HBsAg antigen reacted with the magnetosomes complex, the obtained detection complex was washed by magnetic separation method, resuspended, and then transferred to the microplate containing the main mixture of PCR to realize the PCR detection of immobilized antigen. The linear detection range was 200 ng mL⁻¹ – 320 pg mL⁻¹. Sun et al. constructed a biosensor to detect pefloxacin (PEF) and microcystin LR (MC-LR) in seafood by using antibody-functionalized gold nanorods (GNRs) as signal probes and antigen-ovalbumin (OVA) functionalized magnetosomes as signal amplification probes [139] (Fig. 14C). The antibody-functionalized GNRs and antigen-OVA functionalized magnetosomes could form aggregates of different sizes according to the concentration of the free antigen. With increased free antigen concentration, the number of assembled magnetic bodies would decrease, and the redshift of GNRs longitudinal surface plasmon resonance (LSPR) would also decrease. Therefore, the sensor could selectively detect PEF and MC-LR with this property, and its linear detection range was 1–20 ng mL⁻¹.

Although the research of biosensors based on magnetosomes is relatively less focused, magnetosomes possess the potential to be applied as biosensors. In addition, due to the low biological toxicity, various substances *in vivo* can be detected using magnetosome-mediated

biosensors.

9. Future perspectives

Since their discovery several decades ago, several advancements have been evidenced in exploring the potential of in diverse fields of medicine. To a considerable extent, these composites have become an alternate material to replace synthetic magnetic nanoparticles because of their superior properties, including uniform particle size, high chemical purity, good magnetic properties, low toxicity, and good biocompatibility. However, most MTB in nature are difficult to purify and cultivate; therefore, the yield is the greatest obstacle for the large-scale application of magnetosomes. However, this problem is expected to be solved with the maturity of genetic manipulation techniques (Red/ET homologous recombination technology) and continuous research on the behavior of MTB and the biomineralization of magnetosomes. In an attempt to overcome the problem of self-aggregation of proteins, Rawlings et al. successfully synthesized sophisticated magnetic nanoparticles by immobilizing the magnetosome membrane proteins MmsF and Mms13 on a scaffold protein with the stem-loop coiled-coil structure [140]. This work also provided an important idea for the *in vitro* synthesis of magnetosomes (Fig. 15A). Moreover, magnetic 3D (bio)printing has emerged as one of the promising fields of research, in which superparamagnetic iron oxide nanoparticles are incorporated into the (bio)ink. The printed materials have unique magnetic properties that confer outstanding potential for application in certain specific scenarios. Moreover, it has been proven that superparamagnetic iron oxide nanoparticles affect the behavior of cells under the effect of an external magnetic field [141–144]. Therefore, magnetosome-based 3D bio-printing towards controlling cellular behaviors and enhancing the physiological relevancy of engineered tissues is also one of the application scenarios of magnetosomes. In addition, studies on magnetosomes are primarily held in the validation phase due to a lack of evidence from clinical investigations. Therefore, studies on the *in vivo* stability, aggregation, and degradation of magnetosomes are required for their substantial scale-up and translation to clinics.

Despite the progress on the biomineralization of intracellular magnetosomes in MTB that has been made in determining different steps and possible precursor stages, elucidation of these mechanisms is an essential guide for applying magnetic nanoparticles. The protein–surface interactions play a prominent role in biomineralization and deposition reactions, and understanding them is crucial. Notably, the biomineralization of MTB provides a good model system. Pohl et al. used single-molecule force spectroscopy with an atomic force microscope. They discovered a magnetic binding protein, Mad10, which could inhibit the growth of these crystalline surfaces and thereby break the symmetry of the nanoparticles [145]. These results indicated the kinetic nature of protein–surface interactions (Fig. 15B). In addition, with the continuous development of material preparation technologies, multidimensional nanomaterials have shown great potential for applications in various fields. From various types of metallic nanowire materials to the classical two-dimensional (2D) nanomaterial graphene, these multidimensional nanomaterials have a wide range of applications in energy conversion, sensing, and biomedicine due to their unique mechanical, optical, electrical, physical, and chemical properties. Moreover, magnetosome chains have been reported to have better performance and applicability than single magnetosomes. Magnetic 2D nanomaterials are mainly obtained by creating vacancies in non-magnetic 2D nanomaterials or by elemental doping. However, the magnetic property of these magnetic 2D nanomaterials is weak and cannot be tuned precisely. In recent years, 2D nanomaterials with intrinsic magnetic properties have been obtained through mechanical exfoliation. Nevertheless, these processes are tedious and complicated, limiting the development of magnetic 2D nanomaterials. Therefore, with the gradual elucidation of the mineralization mechanism of magnetosomes and the continuous development of genetic engineering technology, it is possible to produce long-range,

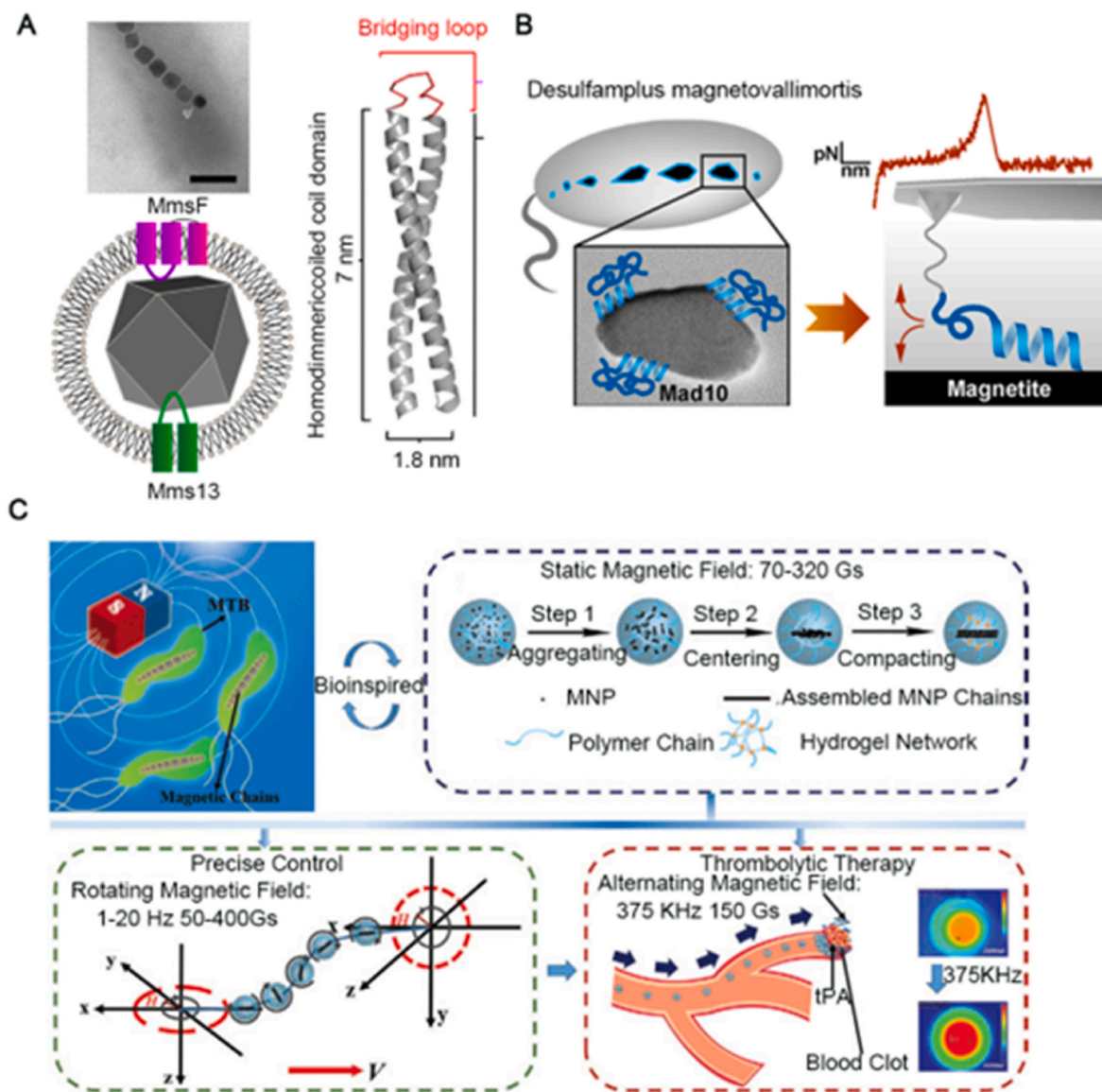


Fig. 15. Advances in the study of magnetosomes and MTB (A) Design and characterisation of coiled coil proteins [143]. Copyright 2019, Nature (B) Illustration of mad10 polypeptide affecting magnetosome crystal growth [144]. Copyright 2019, American Chemical Society (C) Schematic representation of the biomimetic magnetic microrobot (BMM) with magneto-collective regulation for targeted thrombolysis. Magnetosomes in MTB act as the compass to respond to the geomagnetic field. Iron oxide nanoparticle (MNP) assembled into chain-like structures in microgels, similarly to magnetosomes after exposure to an external static magnetic field. The hydrogel shell provided a biocompatible surface matrix and the MNP chains played a role in propulsion and navigation. The BMM could be individually and collectively controlled and driven by the external rotating magnetic field to generate speedy motion response with accurate positioning. The tissue plasminogen activator (tPA)-loaded BMM swarm demonstrated enhanced collective functions under an alternating magnetic field [147]. Copyright 2020, Wiley.

ordered, magnetic 2D nanomaterials using MTB.

Bacteria-mediated carriers can deliver specific drugs (proteins and DNA) into cells through a process termed ‘bacterial infection’ and act as a ‘micro/nano-robot’ to deliver drugs to sites that are difficult to reach with ordinary nanocarriers. MTB have attracted the interest of many researchers because of their magnetotactic characteristics and ability to find low-oxygen regions. Felfoul et al. studied the flagellated marine coccus *Magnetococcus marinus* strain MC-1, indicating that these bacteria possessed self-propelled properties suitable for efficient movement in the microvascular interstitium, angiogenic networks and solid tumors [146]. They accumulated in specific areas through magnetotactic control and their microaerobic behavior. Xing et al. developed a continuous magnetically driven, optically triggered bio-micro-robot that connected indocyanine green nanoparticles with *Magnetospirillum magneticum* strain AMB-1 via Michael addition [147]. The bio-micro-robot displayed magnetic anaerobic behavior and could be enriched at tumor sites,

enabling a multifunctional platform that integrated targeting, PTT, imaging, and diagnosis. Bionic magnetic micro-robots based on MTB have been explored. Xie et al. prepared a ‘micro-robot’ with precise magnetic-collective control, which showed excellent motion and collective transport capability. Accordingly, these studies elucidated the scope for the broad application of magnetosomes in ultra-minimally invasive surgery and drug delivery (Fig. 15C) [148].

In conclusion, MTB and magnetosomes have promising applications in several biomedical fields. With the increasing development of molecular manipulation technology, there has been a focus on modifying magnetosomes at the molecular level and creating various magnetosome nanoplateforms with special functions. These developments will also enhance precision medicine in the future. Nevertheless, the most exciting and challenging idea is whether we can design and manufacture magnet nanotubes using magnetosomes with natural chain structures in magnetotactic bacteria. Since we have seen the outstanding

achievements of carbon nanotubes, we expect that the magnet nanotubes can be used in broader fields such as electromagnetics, signal capture, orbit transportation, interstellar communication as well as biomedical applications, due to their specialized structure and potential electromagnetic properties in the tunnel. We believe that magnetosomes, a natural magnetic nanomaterial that integrates magnetism, biomedicine, and mineralogy, can become a breakthrough in biomedicine.

Statement

This paper does not cover studies in human subjects or animal studies.

Declaration of competing interest

Authors do not have any conflicts of interest to declare.

Acknowledgement

We gratefully acknowledge financial support from the National Natural Science Foundation of China (32171337) and the National Marine Economic Innovation and Development Project (16PYY007SF17). This research was also supported by the Program for Innovative Research Team in Science and Technology at Fujian Province University. We also thank the Instrumental Analysis Center of Huaqiao University for the support of the work. YSZ is not supported by any of these funds; instead, the support by the Brigham Research Institute is thanked.

References

- [1] K.P. Kubelick, M. Mehrmohammadi, *Theranostics* 12 (4) (2022) 1783–1799.
- [2] H.-V. Tran, N.M. Ngo, R. Medhi, et al., *Materials* 15 (2) (2022) 503.
- [3] K. Grünberg, E.-C. Müller, A. Otto, et al., *Appl. Environ. Microbiol.* 70 (2004) 1040–1050.
- [4] D. Schüler, *FEMS (Fed. Eur. Microbiol. Soc.) Microbiol. Rev.* 32 (4) (2008) 654–672.
- [5] S. Bellini, *Chin. J. Oceanol. Limnol.* 27 (2009) 6–12.
- [6] R. Blakemore, *Science* 190 (1975) 377–379.
- [7] T. Yoshino, H. Hirabe, M. Takahashi, et al., *Biotechnol. Bioeng.* 101 (3) (2008) 470–477.
- [8] P. Tajer-Mohammad-Ghazvin, R. Kasra-Kermanshahi, A. Nozad-Golikand, et al., *Bioproc. Biosyst. Eng.* 39 (12) (2016) 1899–1911.
- [9] W. Lin, Y. Pan, *Mol. Microbiol.* 82 (6) (2011) 1301–1314.
- [10] Y. Maeda, T. Yoshino, M. Takahashi, et al., *Appl. Environ. Microbiol.* 74 (16) (2008) 5139–5145.
- [11] S. Meriaux, M. Boucher, B. Marty, et al., *Adv. Healthc. Mater.* 4 (7) (2015) 1076–1083.
- [12] L. Yuan, M. Xie, S. Wang, Q. Zheng, et al., *Mater. Lett.* 100 (2013) 248–251.
- [13] Q. Dai, R. Long, S. Wang, et al., *Microb. Cell Factories* 16 (1) (2017) 216.
- [14] L. Cheng, Y. Ke, S. Yu, et al., *Int. J. Nanomed.* 11 (2016) 5277–5286.
- [15] A.S. Mathuriya, *Biotechnol. Lett.* 37 (3) (2015) 491–498.
- [16] E. Alphandéry, I. Chebbi, F. Guyot, et al., *Int. J. Hyperther.* 29 (8) (2013) 801–809.
- [17] K. Xiong, W. Wei, Y. Jin, et al., *Adv. Mater.* 28 (36) (2016) 7929–7935.
- [18] R.P. Blakemore, D. Maratea, R.S. Wolfe, *J. Bacteriol.* 140 (1979) 720–729.
- [19] U. Heyen, D. Schüler, *Appl. Microbiol. Biotechnol.* 61 (5) (2003) 536–544.
- [20] Y. Zhang, X. Zhang, W. Jiang, et al., *Appl. Environ. Microbiol.* 77 (17) (2011) 5851–5856.
- [21] F.C. Alfred, H. Li, O. Thomas, et al., *N. Biotech.* 46 (2018) 22–30.
- [22] C. Berny, R. Le Fèvre, F. Guyot, et al., *Front. Bioeng. Biotechnol.* 8 (2020).
- [23] D. Faivre, D. Schuler, *Chem. Rev.* 108 (2008) 4875–4898.
- [24] C.T. Lefèvre, D.A. Bazylinski, *Microbiol. Mol. Biol. Rev.* 77 (3) (2013) 497–526.
- [25] T. Islam, C. Peng, L.J. Ali, *J. Basic Microbiol.* 58 (5) (2017) 1–12.
- [26] O. Raschdorf, Y. Forstner, I. Kolinko, et al., *PLoS Genet.* 12 (2016), e1006101.
- [27] D. Yamamoto, A. Taoka, T. Uchihashi, et al., *Proc. Natl. Acad. Sci. U.S.A.* 107 (2010) 9382–9387.
- [28] B.L. Dubbels, A.A. Dispirito, J.D. Morton, et al., *Microbiology* 150 (2004) 2931–2945.
- [29] D. Faivre, L.H. Bottger, B.F. Matzanke, et al., *Angew. Chem. Int. Ed.* 46 (2007) 8495–8499.
- [30] R.J. Calugay, H. Takeyama, D. Mukoyama, et al., *J. Biosci. Bioeng.* 101 (2006) 445–447.
- [31] M.I. Siponen, P. Legrand, M. Widdrat, et al., *Nature* 502 (2013) 681–684.
- [32] W. Niu, Y. Zhang, J. Liu, *Free Radic. Biol. Med.* 161 (2020) 272–282.
- [33] M. Tanaka, E. Mazuyama, A. Arakaki, et al., *J. Biol. Chem.* 286 (2011) 6386–6392.
- [34] D. Faivre, T.U. Godec, *Angew. Chem. Int. Ed.* 54 (2015) 4728–4747.
- [35] A. Arakaki, A. Yamagishi, A. Fukuyo, et al., *Mol. Microbiol.* 93 (2014) 554–567.
- [36] A. Scheffel, M. Gruska, D. Faivre, et al., *Nature* 440 (2006) 110–114.
- [37] A. Scheffel, D. Schuler, *J. Bacteriol.* 189 (2007) 6437–6446.
- [38] W. Pan, C. Xie, J. Lv, *Curr. Microbiol.* 64 (2012) 515–523.
- [39] M. Toro-Nahuelpan, G. Giacomelli, O. Raschdorf, et al., *Nat. Microbiol.* 4 (11) (2019) 1978–1989.
- [40] I. Medalsy, O. Dgany, M. Sowwan, et al., *Nano Lett.* 8 (2008) 473–477.
- [41] S. Behrens, A. Heyman, R. Maul, et al., *Adv. Mater.* 21 (2009) 1–5.
- [42] C. Lang, D. Schuler, *Appl. Environ. Microbiol.* 74 (2008) 4944–4953.
- [43] F. Mickoleit, C. Lanzloth, D. Schüler, *Small* 16 (16) (2020), 1906922.
- [44] N. Ginet, R. Pardoux, G. Adryanczyk, et al., *PLoS One* 6 (6) (2011) 1–7.
- [45] M. Furubayashi, A.K. Wallace, *Adv. Funct. Mater.* 31 (2021), 2004813.
- [46] E.R. Goldman, G.P. Anderson, P.T. Tran, et al., *Anal. Chem.* 74 (2002) 841–847.
- [47] X. Gao, Y. Cui, R.M. Levenson, et al., *Nat. Biotechnol.* 22 (2004) 969–976.
- [48] D.S. Grubisha, R.J. Lipert, H.Y. Park, et al., *Anal. Chem.* 75 (2003) 5936–5943.
- [49] T. Mirzabekov, H. Kontos, M. Farzan, et al., *Nat. Biotechnol.* 18 (2000) 649–654.
- [50] T. Tanaka, H. Takeda, Y. Kokuryu, et al., *Anal. Chem.* 76 (2004) 3764–3769.
- [51] F. Pi, J. Sun, W. Liu, et al., *Food Control* 80 (2017) 319–326.
- [52] A. Jij, B. Sk, *Biotechnol. Rep.* 25 (2020), e00422.
- [53] Q.J. Deng, Y.G. Liu, S.B. Wang, *Sci. Bull.* 59 (2014) 945–952.
- [54] J.B. Sun, J.H. Duan, S.L. Dai, et al., *Biotechnol. Bioeng.* 101 (2008) 1313–1320.
- [55] L. Guo, J. Huang, L.M. Zheng, et al., *Nanotechnology* 22 (2011), 175102.
- [56] Y. Liu, Q. Dai, S. Wang, et al., *Int. J. Nanomed.* 10 (2015).
- [57] J. Li, Y. Pan, Q. Liu, et al., *Earth Planet Sci. Lett.* 293 (3–4) (2010) 368–376.
- [58] U. Heyen, D. Schüler, *Appl. Microbiol. Biotechnol.* 61 (5) (2003) 536–544.
- [59] J.L.&Y. Panab, *Geomicrobiol. J.* 29 (4) (2012) 362–373.
- [60] S. Borg, D. Rothenstein, J. Bill, et al., *Small* 11 (2015) 4209–4217.
- [61] A. Kobayashi, J.L. Kirschvink, C.Z. Nash, et al., *Earth Planet Sci. Lett.* 245 (3–4) (2006) 538–550.
- [62] M. Molcan, H. Gojzewski, A. Skumiel, et al., *J. Phys. Appl. Phys.* 49 (36) (2016), 365002.
- [63] Liu Rui-ting, Jie Liu, Jie-qiong Tong, et al., *Prog. Nat. Sci.: Mater. Int.* 22 (1) (2012) 31–39.
- [64] J. Sun, T. Tang, J. Duan, et al., *Nanotoxicology* 4 (3) (2010) 271.
- [65] T. Revathy, M.A. Jayasri, K. Suthindhiran, *3 Biotech* 7 (2) (2017) 126.
- [66] L. Yan, Yue, et al., *Materials Science and Engineering, C*, 2012.
- [67] V. Raguraman, K. Suthindhiran, *Int. J. Environ. Health Res.* (2019) 1–13.
- [68] L. Qi, X. Lv, T. Zhang, et al., *Sci. Rep.* 6 (2016), 26961.
- [69] F. Mickoleit, C. Jrke, S. Geimer, et al., *Nanoscale Adv.* 3 (2021) 3799–3815.
- [70] B. Xia, T.C. Yan, D. Jt, et al., *Toxicology* 462 (2021), 152949.
- [71] J.H. Gao, H. Lei, Q. Chen, et al., *Scientia Sinica Vitae* 50 (2020) 1285–1295.
- [72] J. Wahsner, E.M. Gale, A. Rodríguez-Rodríguez, et al., *Chem. Rev.* 119 (2018) 957–1057.
- [73] Y. Cai, Y. Wang, H. Xu, et al., *Nanoscale* 6 (2019) 2644–2654.
- [74] Zijian Zhou, Lijiao Yang, Jinhao Gao, et al., *Adv. Mater.* 31 (2019), 1804567.
- [75] L.L. Zhang, F.F. Zhang, Z. Wang, X.F. You, et al., *IEEE Trans. Appl. Supercond.* 22 (3) (2010) 822–825.
- [76] Y. Zhang, Q. Ni, C. Xu, et al., *ACS Appl. Mater. Interfaces* 11 (2018) 3654–3665.
- [77] B. Zheng, T. Vazin, P. Goodwill, et al., *Sci. Rep.* 5 (2015), 14055.
- [78] B. Zheng, M.P. von See, E. Yu, et al., *Theranostics* 6 (2016) 291–301.
- [79] F. Fidler, M. Steinke, A. Kraupner, et al., *IEEE Trans. Magn.* 51 (2015) 1–4.
- [80] R. Orendorff, M. Wendland, E. Yu, et al., *World Molecular Imaging Congress (WMIC 2016)*, 2016, 2016.
- [81] X.Y. Zhou, K. Jeffris, E. Yu, et al., *Phys. Med. Biol.* 62 (2017) 3510–3522.
- [82] J. Haegele, J. Rahmer, B. Gleich, et al., *Radiology* 265 (2012) 933–938.
- [83] E.Y. Yu, M. Bishop, B. Zheng, et al., *Nano Lett.* 17 (2017) 1648–1654.
- [84] Z.W. Tay, P. Chandrasekharan, Andreina Chiu-Lam, et al., *ACS Nano* 12 (4) (2018) 3699–3713.
- [85] G. Song, X. Zheng, Y. Wang, et al., *ACS Nano* 13 (7) (2019) 7750–7758.
- [86] D. Heinke, A. Kraupner, D. Eberbeck, et al., *Infinite Science Publishing* 3 (2) (2017), 1706004.
- [87] A. Jz, A. Jc, A. Sm, et al., *Acta Pharm. Sin.* B 8 (3) (2018) 320–338.
- [88] S. Kurbegovic, K. Juhl, H. Chen, et al., *Bioconjugate Chem.* 29 (11) (2018) 3833–3840.
- [89] H.-W. An, D. Hou, R. Zheng, et al., *ACS Nano* 14 (1) (2020) 927–936.
- [90] H.D. Li, Q.C. Yao, W. Sun, et al., *J. Am. Chem. Soc.* 142 (13) (2020) 6381–6389.
- [91] L. Wu, A.C. Sedgwick, X. Sun, et al., *Acc. Chem. Res.* 52 (9) (2019) 2582–2597.
- [92] E. Alphandéry, D. Abi Haidar, Seksek Olivier, et al., *Nanoscale* 10 (2018), 10918.
- [93] D. Faivre, D. Schüler, *Chem. Rev.* 108 (2008) 4875–4898.
- [94] P.S. Patrick, L.K. Bogart, T.J. Macdonald, et al., *Chem. Sci.* (2019).
- [95] H. Lin, Y. Chen, J. Shi, *Chem. Soc. Rev.* 47 (2018) 1938–1958.
- [96] B. Xue, Y. Zhang, M. Xu, et al., *J. Biomed. Nanotechnol.* 15 (4) (2019) 769–778.
- [97] M. Xu, G. Li, H. Zhang, et al., *Drug Deliv.* 27 (1) (2020) 983–985.
- [98] F.E. Kong, G.M. Li, Y.Q. Tang, et al., *Sci. Transl. Med.* 13 (579) (2021), eabb6282.
- [99] S.-Y. Li, H. Cheng, B.R. Xie, et al., *ACS Nano* 11 (2017) 7006–7018.
- [100] Y. Zhang, Q. Ni, C. Xu, et al., *ACS Appl. Mater. Interfaces* 11 (2019) 3654–3665.
- [101] F. Wang, C. Chen, Y. Chen, et al., *Colloids Surf. B Biointerfaces* 172 (2018) 308–314.
- [102] A.P. Sangnier, S. Preveral, A. Curcio, et al., *J. Contr. Release* 279 (2018) 271–281.
- [103] J. Sun, Y. Li, X.J. Liang, et al., *J. Nanomater.* 2011 (2011) 469031–469043.
- [104] V. Raguraman, K. Suthindhiran, *IET Nanobiotechnol.* 14 (9) (2020) 815–822.
- [105] R.M. Long, Q.L. Dai, X. Zhou, et al., *Int. J. Nanomed.* 13 (2018) 8269–8279.
- [106] R. Long, Y. Liu, Q. Dai, et al., *Materials* 9 (11) (2016) 889.

- [107] Z. Wang, *Nano Today* 35 (1) (2020), 100946.
- [108] Z. Chen, B. Wenbo, N. Dalong, et al., *Angew. Chem. Int. Ed.* 55 (2016) 2102–2106.
- [109] P. Wei, Chia H. Li, et al., *ACS Nano* 10 (2) (2016) 2017–2027.
- [110] X. Liu, Y. Zhang, Y. Wang, et al., *Theranostics* 10 (8) (2020) 3793–3815.
- [111] E. Alphanđéry, A. Idbah, C. Adam, et al., *Biomaterials* 141 (2017) 210–222.
- [112] E. Alphanđéry, A. Idbah, C. Adam, et al., *J. Contr. Release* (2017) 262.
- [113] Y.F. Zhang, G.L. Li, X. Gao, et al., *ACS Biomater. Sci. Eng.* 6 (2020) 6652–6660.
- [114] R.A. Suriyanto, E.Y.K. Ng, S.D. Kumar, *Biomed. Eng. Online* 16 (2017) 36.
- [115] J. Beik, Z. Abed, F.S. Ghoreishi, et al., *J. Contr. Release* (2016) 205–221.
- [116] D. Han, B.-L. Zhang, L.-C. Su, et al., *J. Mater. Eng.* 47 (4) (2019) 84–90.
- [117] R. Hergt, R. Hiergeist, M. Zeisberger, et al., *J. Magn. Magn. Mater.* 293 (1) (2005) 80–86.
- [118] M. Abdellahi, M. Tajally, O. Mirzaee, *J. Magn. Magn. Mater.* 530 (10) (2021), 167938.
- [119] D. Gandia, L. Gandarias, *Small* 15 (2019), 1902626.
- [120] E. Alphanđéry, S. Faure, L. Raison, et al., *J. Phys. Chem. C* 115 (1) (2011) 18–22.
- [121] E. Alphanđéry, F. Guyot, I. Chebbi, *Int. J. Pharm.* 434 (1–2) (2012) 444–452.
- [122] R. Le Fèvre, D.D. Mickaél, C. Imène, et al., *Theranostics* 7 (18) (2017) 4618–4631.
- [123] C. Mandawala, I. Chebbi, M. Durand-Dubief, et al., *J. Mater. Chem. B* 10 (2017) 1039.
- [124] G. Li, J. Wang, M. Xu, et al., *Appl. Mater. Today* 20 (2020), 100723.
- [125] J. Wang, G. Li, C. Tu, et al., *Nanoscale* 12 (25) (2020) 13742–13756.
- [126] M. Xu, G. Li, H. Zhang, et al., *Drug Deliv.* 27 (1) (2020) 983–995.
- [127] S. Liu, X. Pan, H. Liu, *Angew. Chem. Int. Ed.* 59 (2020) 5890–5900.
- [128] Y. Peng, F. Li, J. Zou, *Adv. Funct. Mater.* 32 (17) (2022), 2110063.
- [129] T.J. Yu, P.H. Li, T.W. Tseng, et al., *Nanomedicine* 6 (8) (2011) 1353–1363.
- [130] G. Yuan, Y. Yuan, K. Xu, et al., *Int. J. Mol. Sci.* 15 (10) (2014) 18776–18788.
- [131] C. Chen, S. Wang, L. Li, et al., *Biomaterials* 104 (2016) 352–360.
- [132] M. Binnewies, E.W. Roberts, K. Kersten, et al., *Nat. Med.* 24 (2018) 541–550.
- [133] M.F. Sanmamed, L. Chen, *Cell* 175 (2018) 313–326.
- [134] Fan Zhang, Feng Li, Gui-Hong Lu, et al., *ACS Nano* 13 (2019) 5662–5673.
- [135] Q. Zhang, W. Wei, P. Wang, et al., *ACS Nano* 11 (2017) 10724–10732.
- [136] L. Wu, B. Gao, F. Zhang, et al., *Talanta* 106 (2013) 360–366.
- [137] Y. Amemiya, T. Tanaka, B. Yoza, et al., *J. Biotechnol.* 120 (3) (2005) 308–314.
- [138] R. Wacker, B. Ceyhan, P. Alhorn, et al., *Biochem. Biophys. Res. Commun.* 357 (2) (2007) 391–396.
- [139] X. Sun, L. Wu, J. Ji, et al., *Biosens. Bioelectron.* 47 (2013) 318–323.
- [140] A.E. Rawlings, L.A. Somner, M. Fitzpatrick-Milton, et al., *Nat. Commun.* 10 (1) (2019) 2873.
- [141] B. Yzza, C.B. Rui, B. Ppx, et al., *Mater. Sci. Eng. C* 122 (2021), 11877.
- [142] J.M. Lee, W.Y. Yeong, *Adv. Healthc. Mater.* 5 (22) (2016) 2856–2865.
- [143] B. Hyla, B. Hyh, C. Sjs, et al., *J. Magn. Magn. Mater.* 504 (2020), 166680.
- [144] E. Tanasa, C. Zaharia, A. Hudita, et al., *Mater. Sci. Eng. C* 110 (2020), 110714.
- [145] A. Pohl, F. Berger, R. M, et al., *Nano Lett.* 19 (11) (2019) 8207–8215.
- [146] O. Felfoul, M. Mohammadi, S. Taherkhani, et al., *Nat. Nanotechnol.* 11 (11) (2016) 941–947.
- [147] J. Xing, T. Yin, S. Li, et al., *Adv. Funct. Mater.* 31 (2021), 2008262.
- [148] M. Xie, W. Zhang, C. Fan, et al., *Adv. Mater.* (2020), 2000366.